UNIVERSITÀ
di VERONA

Department of Diagnostics and Public Health

A Dissertation presented

By

PhD Candidate:

Anastasios Gkountakos

Assessing the potential role of *Rictor* expression as predictive factor of response to PI3K/mTOR pathway inhibitors in preclinical models of Squamous Cell Lung Cancer

S.S.D. (Disciplinary Sector): MED\08

Submitted to the Graduate school of Life and Health Sciences
PhD Program in Inflammation, Immunity and Cancer
XXXII Cycle

Coordinator***: Prof. Gabriela Constantin***

Tutor: ***Prof. Aldo Scarpa***

PhD candidate: **Anastasios Gkountakos**

I, Anastasios Gkountakos, confirm that the work presented here in this thesis is my own. Where information has been derived from other sources, I declare that it has been indicated appropriately.

I authorize any physical person to consult and copy part of this thesis for personal use only, concerning the obligation to refer to the source whenever and wherever material from this thesis are cited.

Acknowledgements

I would like to express my gratitude to my tutor, professor Aldo Scarpa for giving me the opportunity to perform my PhD Thesis in his exceptional laboratory facilities.

I would like also to greatly thank professor Emilio Bria for his constant support throughout these years.

I am grateful to assistant professor Vincenzo Corbo and privileged to have met him. Over the last years, his brilliant guidance kept my project always on the right path and focused on meaningful targets.

I owe a special thanks to all the people in the lab and department for the fruitful collaboration we had these years.

From the bottom of my heart, I wish everyone the best.

Anastasios Gkountakos

Κι αν πτωχική την βρεις, η Ιθάκη δεν σε γέλασε.
Έτσι σοφός που έγινες, με τόση πείρα,
ήδη θα το κατάλαβες η Ιθάκες τι σημαίνουν.

Κωνσταντίνος Π. Καβάφης, 1911

Στον πατέρα μου

Table of Contents

Abstract

Squamous cell lung cancer (SQLC) is the second most prevalent histologic type of lung cancer and accounting for approximately 30% of newly diagnosed non-small cell lung cancer (NSCLC) cases. Systemic treatments for SQLC patients include cytotoxic chemotherapy and immune-oncology approaches. In contrast with lung adenocarcinoma, which is the other main subtype of NSCLC, no patient-tailored treatments are available so far for SQLC. Accumulating evidence suggests that the PI3K/mTOR axis is one of the most frequently altered pathways in SQLC. However, despite a plethora of clinical trials with numerous PI3K/mTOR targeted inhibitors, no significant increase in patients' survival has been observed as compared to standard treatment options. A possible explanation for the outcome of those clinical trials might be the lack of reliable predictive biomarkers for better patients' stratification.

We and others have reported *Rictor* copy number gain (CNG) in a set of SQLC patients by performing targeted DNA sequencing on archival tissues. Another group has suggested the existence of *Rictor* focal amplification in subsets of lung cancers, including SQLC, and further suggested *Rictor* as a potential predictive biomarker of response to targeted therapy.

However, no conclusive data were presented to show that *Rictor* amplification is driving activation of the PI3K/mTOR pathway in SQLC cells or representing a valid biomarker predictive of response to targeted inhibition of the pathway.

Here, we used three different SQLC cell lines and 60 tissue specimens to show that CNG of *Rictor* is a recurrent event in SQLC, yet this is due to the polysomy of the short arm of chromosome 5 rather than to focal amplification. All three cell lines tested showed different *Rictor* CNG and different levels of its transcript and protein. In particular, the SQLC cell line harboring the higher CNG (H-1869) accordingly displayed higher level of Rictor protein. Therefore, we sought to test the possibility that the dosage of Rictor might affect the activation of PI3K/mTOR pathway and sensitivity towards its targeting agents. Unexpectedly, we found that Rictor levels did not parallel the biochemical activation of the

pathway nor the sensitivity to dual mTORC1/C2 or PI3K/mTOR inhibitions. These observations were confirmed by genetic perturbation analysis, as reduction of Rictor levels through RNA interference did not lead neither to reduced cell viability nor to significant changes in drug sensitivity in the two cell lines tested. Overall, our findings suggest that Rictor does not represent a predictive biomarker of response towards PI3K/mTOR directed therapy.

List of Figures

List of Tables

1 Introduction

1.1 Lung cancer in 2020

Lung cancer is one of the most frequent cancer types and the leading cause of cancer-related deaths for both genders **(Fig. 1.1)**. Identified risk factors tightly associated with lung cancer development include tobacco consumption, second-hand smoking, and long-term inhalation of toxic substances [1]. The global epidemiology of lung cancer is also associated with geographical and socioeconomical characteristics [2]. Initial classification of lung cancer is based on the histological type and distinguishes between small cell lung cancer (SCLC) and non-small cell lung cancer (NSCLC). NSCLC accounts for approximately 80% of new lung cancer diagnosis, with lung adenocarcinoma (LUAD) and squamous cell lung carcinoma (SQLC) representing 40% and 30% of the cases, respectively [3]. At the time of diagnosis, the majority of patients suffer from distant metastasis, which leads to poor survival rates. Although lung cancer mortality has been decreasing over the past decade, likely due to recent advances in lung cancer treatment such as the advent of targeted therapies and immunotherapy, the therapeutic armamentarium for SQLC patients is still lacking reliable patient-tailored treatments [4]. Therefore, development of more personalized therapeutic approaches to treat SQLC is urgently required.

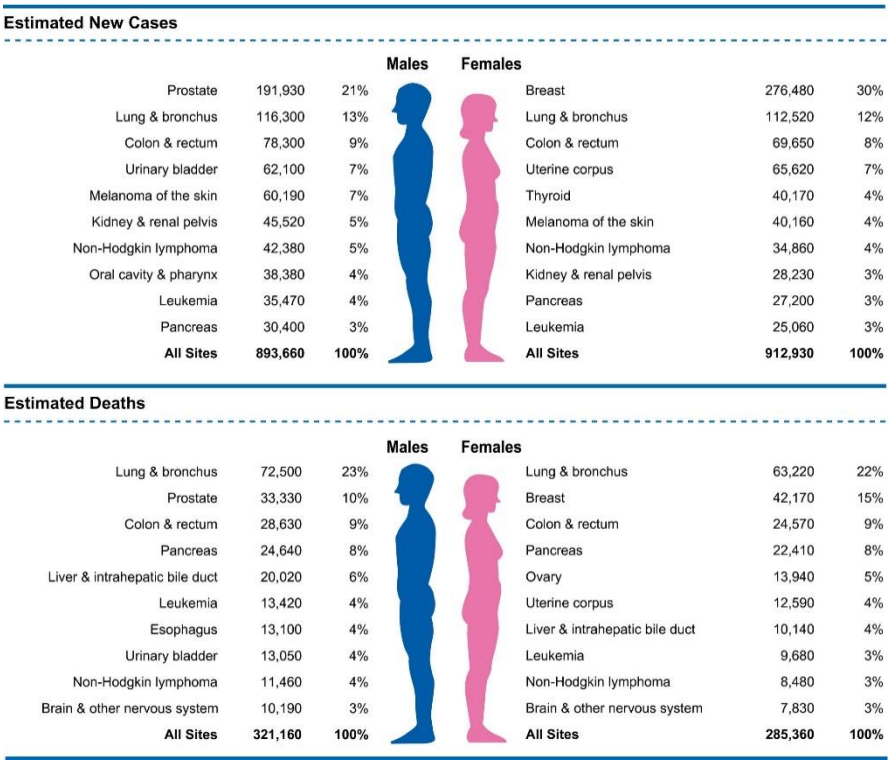

Figure 1.1. Cancer type incidences and mortality rates for both genders, United States of America 2020

Lung cancer is one of the most common cancer types and the leading cause of cancer-related death accounting approximately for one-quarter of them overall. Data from Siegel et al. [4].

1.2 Squamous Cell Lung Cancer

SQLC represents the 25-30% of newly diagnosed NSCLC cases and is highly associated with tobacco smoking. SQLC is usually a centrally located tumor mass close to the hilum of the lung. While the cellular origin of lung cancer is largely unknown, studies in available mouse SQLC models suggest that SQLC might originates from Keratin5^{+}/Keratin14^{+}/p63^{+} tracheal basal cell progenitors, which present stem cell characteristics [5]. Today it is widely accepted that the histologic progression towards the SQLC establishment involve a primary, generalized basal cell hyperplasia, followed by squamous metaplasia, dysplasia, carcinoma in situ, and, eventually, the development of invasive SQLC disease [6]. Histological differences between SQLC and LUAD assist pathologists to diagnose accurately patients' lung cancer subtypes. P63 is a transcription factor and validated diagnostic indicator, ubiquitously expressed in SQLC. Other validated discriminators of SQLC from LUAD is p40 and cytokeratin 5/6 [7,8]. In 2015, World Health Organization (WHO) updated SQLC classification with important changes from the

previous classification. The new classification identifies three subtypes of SQLC, which are the keratinizing, nonkeratinizing and basaloid subtypes [3]. Besides histological subclassification, with the advent of high-throughput sequencing technologies, attempts to molecularly classify SQLC became more frequent. Perez-Moreno et al. [9], classified molecular alterations according to their therapeutic targets in three main categories.

- Membrane Receptor Alterations: Fibroblast growth factor 1 (FGFR1), Discoidin Domain Receptor 2 (DDR2), MET, ERBB2/Her2.
- Signaling pathway alterations: Phosphoinositide 3-kinase catalytic a (PI3KCA), Akt1, Phosphatase and Tensin homolog (PTEN), BRAF, EML4-ALK, STK11/LKB1
- Transcription Factor alterations: p53, Sex-determining region Y-Box 2(SOX2) [9]

In the following table, the frequency of the most common genetic alterations reported in SQLC and LUAD is presented, rendering clear the large genetic inconsistency between these two subtypes of lung cancer (**Table 1.1**).

Genetic abnormality	Gene location	SCC	Adenocarcinoma
TP53	17p13.1	51%	36%
PI3KCA amplification	3q26.3	33%	6%
SOX2 amplification	3q26.3-q27	23%	Very rare
FGFR1 amplification	8p12	22%	1%
PTEN mutation	10q23.3	10%	2%
MET amplification	7q31.1	3%–21%	3%–21%
PTEN loss	10q23.3	8%–20%	8%–20%
KRAS mutation	12p12.1	6%	21%
Variant III mutation	7p12	5%	Very rare
LKB1 mutation	19p13.3	5%	23%
DDR2 mutation	1q23.3	4%	1%
HER2 overexpression	17q11.2-q12, 17q21	3%–5%	5%–9%
PI3KCA mutation	3q26.3	3%	3%
BRAF mutation	7p34	2%	1%–3%
EGFR mutation	7p12	<5%	10%–15%
AKT1 mutation	14q32.32	1%	Very rare
MET mutation	7q31.1	1%	2%
HER2 mutation	17q11.2-q12, 17q21	1%	2%
EML4-ALK fusion	2p21, 2p23	1%	2%–7%

Table 1.1. Frequency of the most common molecular alterations in SQLC and comparison with LUAD. Data from Perez-Moreno et al. [9].

A recent classification of SQLC was suggested by an integrative study involving DNA copy number, somatic mutations, RNA sequencing, and expression proteomics in a cohort of 108 SQLC patients, which identified three proteomic subtypes, with two of them (Inflamed and Redox) accounting for 87% of tumors. Tumors belonging to the Inflamed category were enriched with neutrophils, antigen presenting molecules, memory B cells, monocytes and increased PD-1 mRNA

expression than the other two subtypes. The other subtype, Redox, is enriched for oxidation-reduction and glutathione pathways. These findings are appealing and prompt new studies to test immunotherapy and metabolic drugs in those molecular subtypes [10].

1.3 Current Treatment Options for Squamous Cell Lung Cancer

The identification of a subset of lung adenocarcinoma patients harboring EGFR mutations and their treatment with first (gefitinib, erlotinib, icotinib), second (afatinib), and recently third (osimertinib) generation of tyrosine kinase inhibitors [11], divided in a large scale the therapeutic landscape for these two types of lung cancer, providing a great advantage for LUAD patients. For SQLC, the treatment strategies involve only platinum doublet chemotherapeutic schemes and only recently, the introduction of immunotherapy expanded available treatment options. Pembrolizumab, an immune checkpoint inhibitor, initially approved as a second-line therapy, is now administrated as first-line monotherapy or in combination with platinum-based chemotherapy for SQLC patients with 50% or greater PD-L1 expression [12]. However, patients with less than 50% of PD-L1 expression, do not experience increased benefit from pembrolizumab over platinum doublet chemotherapy. Also, nivolumab, another PD-1 inhibitor, failed to prolong OS and PFS compared with standard of care platinum doublet chemotherapy for NSCLC patients according CheckMate 026 study [13].

1.4 Targeted therapy for Squamous Cell Lung Cancer

Despite the quite promising perspective of immunotherapy, a significantly high proportion of SQLC patients can be only treated with chemotherapy. In 2012, The Cancer Genome Atlas (TCGA) consortium reported the comprehensive molecular profiling of 178 resected early stage SQLC patient and identified several potentially druggable alterations [14]. SQLC patients are characterized by TP53 mutations, CDKN2A deletions/mutations, FGFR1 amplification, DDR2 mutations, and PI3KCA amplification and mutations [15,16]. With the regard to the PI3K/mTOR pathway, PI3KCA mutations and amplification can be found in 10% and 40% of SQLC cases, respectively. PTEN loss, detected by IHC, is reported in 24% of cases

while PTEN mutations in 7% of cases [17-19]. Interestingly, both *in vitro* and *in vivo* SQLC models harboring PI3KCA and PTEN alterations exhibited sensitivity to PI3K targeted inhibitors [20]. Interestingly, EGFR exon 19 deletions, EGFR exon 21 L858R mutations and KRAS mutations, all frequent alterations in LUAD, are rare or absent in SQLC [21]. Although numerous potentially druggable alterations have been identified in SQLC patients, to date none of them represent a validated biomarker for targeted therapy. However, clinical guidelines suggest that even SQLC patients having specific clinical characteristics (young age, light/never smokers) should be subjects of molecular testing for identification of targetable alterations [22,23]. Increasing evidences suggest that PI3K/mTOR pathway is one of the most frequently altered pathways in SQLC, and likely represents a driver alteration. However, while more than 40 targeted inhibitors have been developed and many of them have been tested in clinical trials, solid conclusions regarding the potential benefit on survival have not yet achieved. A possible explanation for this situation might be that yet, a reliable predictive biomarker has not been identified [24].

1.5 mTORC1 and mTORC2 complexes

The mTOR is a well-conserved 289 kDa serine/threonine kinase that exists at least in two structurally and functionally distinct multi-protein complexes in mammalian cells, mTOR complex 1 and 2 (mTORC1 and mTORC2). The mTOR kinase is strongly interconnected with the PI3K/Akt axis, as well as with many other crucial pathways, eventually establishing an intricate signaling network. Both complexes share the same central catalytic subcomponent mTOR, the scaffolding protein mammalian lethal with SEC thirteen 8 (mLST8) and the negative regulatory subunit DEP domain-containing mTOR-interacting protein (Deptor) [25,26]. mTORC1 and mTORC2 are defined by the presence of the accessory subunits regulatory-associated protein of mTOR (Raptor) and rapamycin-insensitive companion of mTOR (Rictor), respectively. Furthermore, several components and interacting proteins participate in the assembly, control and activity of the two complexes (**Table 1.2**) [27-30].

	Molecule	mTORC1	mTORC2	Role and Function
Complex components	mTOR	+	+	Ser/Thr protein kinase ▪ Activation of the downstream effectors
	mLST8	+	+	mTOR-interacting protein ▪ Protein-protein interaction ▪ Promotion of mTOR activity
	Deptor	+	+	mTOR-interacting protein ▪ Negative regulator
	Tti1/Tel2	+	+	mTOR-interacting protein ▪ Formation and stability of the complexes
	GRp58	+	+	mTOR-interacting protein ▪ Assembly and activity of mTORC1 ▪ Undefined role for mTORC2
	Raptor	+	-	Scaffold protein ▪ Recognition and recruitment of the downstream effectors
	PRAS40	+	-	Raptor-interacting protein ▪ Negative regulator
	Rictor	-	+	Scaffold protein ▪ Assembly, stability and activity of mTORC2 ▪ Recognition and recruitment of the downstream effectors
	Protor	-	+	Rictor-interacting protein ▪ Undefined role
	mSin1	-	+	mTOR and Rictor-interacting protein ▪ Assembly and activity of mTORC2 ▪ Subcellular localization of the complex
	Hsp70	-	+	Rictor-interacting protein ▪ Assembly and activity of mTORC2
Interacting proteins	Rac1	+	+	mTOR-interacting protein ▪ Localization of the complexes close to the substrates
	XPLN	-	+	mTOR and Rictor-interacting protein ▪ mTORC2 inhibitor
	NBS1	-	+	mTORC2-interacting protein ▪ Participation in the Akt activity
	IKKα	+	+	Raptor and Rictor-interacting protein ▪ Promotion of mTORC1/2 activity
	IKKβ	+	+	Rictor-interacting protein ▪ Promotion of mTORC1/2 activity

Table 1.2. mTOR complex components and their interacting proteins. Data from Gkountakos et al. [31].

mTORC1 senses and responds to a wide array of stimuli, including growth factors, nutrients and environmental stresses. Growth factors and high nutrient availability generally stimulate mTORC1 to promote cell proliferation through favoring anabolic processes and downregulating autophagy. Growth factors are the only well-defined stimulus for mTORC2, which promotes cell survival, proliferation and migration along with actin cytoskeleton reorganization through phosphorylation and activation of downstream kinases including Akt, protein kinase C (PKC) and serum/glucocorticoid-induced kinase 1 (SGK1). While mTORC1 signaling is acutely sensitive to rapamycin, mTORC2 is considered insensitive and only prolonged treatment impairs its function in certain cell lines [32]. The mTORC2 complex is an essential downstream effector of the PI3K signaling pathway and carries out the critical step of Akt activation by phosphorylating the residue S473 on its C-terminal hydrophobic motif. Upon activation, Akt plays a strong oncogenic role by either inducing or inhibiting downstream transcription factors [33]. An overview of the mTORC1/2-Rictor signaling network is presented in **Figure 1.2**.

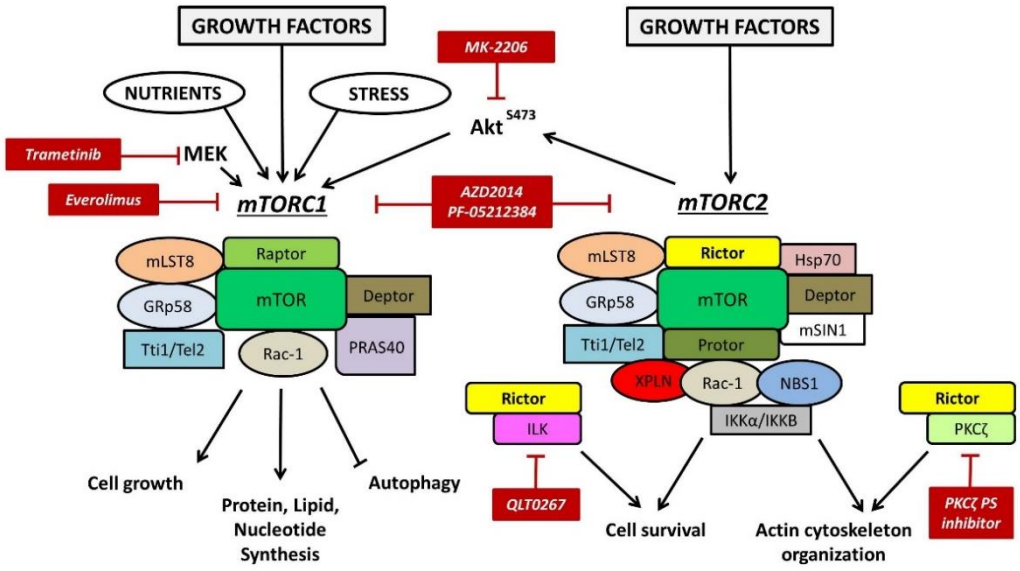

Figure 1.2. Signaling through mTORC1 and mTORC2 in cancer. The mTOR Ser/Thr kinase is the principal catalytic subunit of two distinct multicomponent complexes named as mTORC1 and mTORC2. mTORC1 contains also Raptor, Deptor, PRAS40, mLST8 as well as Tti1/Tel2, GRp58 and Rac-1. Activation of mTORC1 is triggered by different environmental stimuli including growth factors, nutrient availability and stress status. Signaling through mTORC1 regulates the cell growth and promotes the biogenesis of macromolecules while inhibiting the autophagy process. On the other hand, mTORC2 consists of Rictor, Protor, mSIN1, mLST8, Tti1/Tel2 and GRp58, Rac-1, XPLN, NBS1, IKKa/IKKB. In response to growth factors, mTORC2 phosphorylates its downstream substrates Akt, SGK and PKC which are in charge of the cell survival and the actin cytoskeleton remodeling. Rictor associates with other factors establishing complexes with an oncogenic action

independently of mTOR presence. The following compounds are commercially available molecular targeted agents with a potential anti-cancer activity: PF-05212384 (PI3K/mTOR inhibitor), AZD2014 (dual mTORC1/2 inhibitor), Trametinib (MEK inhibitor), Everolimus (mTORC1), MK-2206 (pan-Akt inhibitor), QLT0267 (ILK inhibitor), PKCζ pseudosubstrate inhibitor peptide (PKCζ inhibitor). Data from Gkountakos et al. [31].

1.6 Rictor and Akt S473 phosphorylation: the key oncogenic event

Rictor protein consists of 1.709 amino acids and was initially identified in 2004 as a novel component of the mTORC2 complex [34]. Rictor harbors approximately 37 phosphorylation sites, mainly serine or threonine residues lying in the C-terminal region [35]. Of these phosphorylation sites, Thr1135 was demonstrated to be a growth factor-stimulated and rapamycin-sensitive site as it is targeted directly by ribosomal protein S6 kinase 1 (S6K1), an mTORC1 downstream effector [35]. Although there is concordance among studies that this site is not mandatory for mTORC2 complex assembly, it still remains controversial whether the Thr1135 phosphorylation exerts a regulatory role or is dispensable for modulation of mTORC2 kinase activity [35,36]. Nevertheless, it is widely supported that S6K1-mediated phosphorylation of Rictor-Thr1135 could define a model of a regulatory link between the two mTOR branches. Since the first relevant studies, Rictor was demonstrated to have a crucial role in the phosphorylation events of Akt kinase. Two amino acid residues, T308 and S473, have a critical role in Akt activation, triggering downstream oncogenic mechanisms [33]. Silencing of Rictor in different human cancer cell lines diminished the phosphorylation of the Akt at S473, which is reported to increase kinase activity 4-5 times more than the phosphorylation at T308 alone [37]. In addition, data generated from in vitro experiments in adipocytes concluded that mTORC2-Rictor containing complex mediates the phosphorylation of Akt on S473 [38]. Although mTOR protein assembles into two complexes with distinct components and downstream effectors, they appeared to be reciprocally influenced by feedback loop mechanisms [39]. Treatment of tumor cell lines and rat models with mTORC1 inhibitors induced Akt S473 phosphorylation in a Rictor-dependent manner, likely related to S6K1 inactivation. Genetic silencing of *Rictor* or use of the dual PI3K/mTOR inhibitor NVP-BEZ235 attenuated this effect [40,41].

1.7 Impact of Rictor in cancer

As mTOR, Rictor is essential for the development of mouse embryo. However, *Rictor* null mice die later during development (midgestation) compared to mTOR null mice (around time of implantation) [42]. In addition rictor-deficient mouse embryonic fibroblasts completely lacked phosphorylation of Akt on S473 indicating that mTORC2 is the primary kinase for this Akt residue [42]. Moreover, Rictor is involved in the proper function and morphology of the neurons in murine brain [43,44]. Rictor has been implicated in several diseases including polycystic kidney and benign tumors [45,46]. However, the major amount of evidences originated from malignancies [31].

1.8 Rictor in Lung Cancer

The first evidence for the implication of Rictor in lung cancer was the identification of *Rictor* gene amplification as the only genomic aberration in the lung adenocarcinoma of a never smoker 18 years old male [47]. Treatment of the patient with dual mTORC1/2 inhibitors (CC-223 and MLN0128) provided disease stabilization for more than 18 months [47]. This clinical benefit prompted *in vitro* and *in vivo* experiments that demonstrated the sensitivity of *Rictor*-amplified NSCLC cell lines (one SQLC, H1703 and two LUAD, H-23, H-1734) to both dual mTORC1/2 inhibitors and after *Rictor* genetic silencing, reporting a 5-fold increase in IC50 value of H-1703, suggesting the potential role of Rictor as a druggable target [47]. In this work, amplification of *Rictor* were identified through FISH analysis using a locus-specific probe (Rictor, located on the p arm of chromosome 5) and a control probe spanning the q arm of chromosome 5. Therefore, no definitive proof of a localized amplification of Rictor has been provided so far [47]. The evaluation of the TCGA database derived from next-generation sequencing (NGS) platforms showed that *Rictor* amplification is present in approximately 10% of lung adenocarcinoma and 16% of lung squamous cell carcinomas [14]. In a recent study of lung neuroendocrine tumors comprising different histological subtypes, *Rictor* copy number gains were found in 23.6% of cases [48]. Other cohorts reported a prevalence of Rictor alterations in SCLC ranging from 6% to 14%. In these reports, *Rictor* amplification was almost invariably the only

potentially actionable alteration and negatively affected patients' overall survival (OS) [49-51].

Targeted DNA sequencing identified *Rictor* amplification in around 14% of SCLC patients. Interestingly, genes located near the *Rictor* locus on chromosome 5p13, such as FGF10 and IL7R, were also identified as frequently amplified at sequencing. *Rictor*-amplified SCLC cells showed enhanced migratory activity and the use of mTOR inhibitors restrained this phenotype and strongly inhibited their growth [51].

In a large series of NSCLC patients treated with platinum-based chemotherapy, the *Rictor* genetic variant rs6878291 (A>G), was associated with lower rate of clinical benefit and shorter progression-free survival (PFS) [52]. An assessment of Rictor protein expression, but not its genetic status, was performed in primary and brain metastatic lung adenocarcinoma. An increased Rictor and Rictor/mTOR expression was reported in brain metastases compared to the primary lung adenocarcinoma. Moreover, a trend towards significance has been reported between Rictor expression and higher stage of primary adenocarcinoma. Interestingly, Rictor expression was stronger in adenocarcinoma with a brain metastasis (67%) than in those without (28%) [53]. A recent comprehensive analysis of DNA, RNA and proteins identified PI3K/mTOR/Rictor signaling pathway as a potentially druggable prognostic modulator in resected SQLC [54]. Collectively, all the alterations of Rictor in lung cancer are presented in **Table 1.3**.

Tumor type	*Subtype*	*Rictor positivity % (n)*	*Type of Rictor alteration [technique]*	*Correlation*
Lung	Adenocarcinoma	10.3% (53/515)	Amplification [Integrated TGCA analysis]	NR
	Squamous	15.8% (79/501)		
	Adenocarcinoma	8.4% (61/724)	Amplification [CGP]	
	Squamous	7.4% (8/108)		
	SCLC	14.6% (7/48)		
	Large cell NE	8.7% (2/23)		
	Primary adenocarcinoma	37.0% (25/67)	Overexpression [IHC]	Higher stage in primary adenocarcinoma
	Brain metastasis	60.0% (40/67)		
	SCLC	10.0% (10/98)	Amplification [NGS]	NR
	SCLC	6.0% (3/47) 2.0% (1/47)	Amplification Missense mutation [WES - CNV]	NR
	SCLC	14.0% (6/42)	Amplification [targeted exome sequencing]	Decreased OS
	NE	23.6% (35/148)	CNG [NGS]	NR

Table 1. 3. Rictor expression in lung cancer and correlation with clinicopathological characteristics. Data from Gkountakos et al. [31].

Although PI3K/mTOR pathway is aberrantly uncontrolled in a large spectrum of cancer types, the study of mTORC2 signaling axis and its potential significance in the oncogenic event has been lagged behind. Recent studies nominated activation of the PI3K/mTOR-Rictor signaling pathway, driven by presumed *Rictor* amplification, as a potential therapeutic target in subset of SQLC patients.

1.9 Hypothesis and Aim

Building on the aforementioned data, albeit limited for SQLC, our hypothesis suggests that SQLC patients harboring *Rictor* copy gain might show sensitivity to PI3K/mTOR targeted inhibition. This would imply that increased Rictor dosage leads to higher activity of mTOR signaling pathway which is therefore a dependency in subsets of SQLC. Our aim is rigorously assessing whether Rictor amplification and therefore increased PI3K/mTOR signaling is a true dependency in subsets of SQLC. If that is the case, Rictor might represents a valid predictive biomarker for PI3K/mTOR targeted inhibition. To this aim, we used 3 different

SQLC cell lines and genetic and pharmacological perturbation analyses to verify the role of Rictor in SQLC.

2 Materials and Methods

2.1 Cell Lines

The human SQLC cell lines H-1869, H1703 and SK-Mes-1 were purchased from the American Type Tissue Collection (ATCC, Manassas, VA, USA). H-1703 cells were grown in RPMI 1640 medium (Aurogene s.r.l., Rome, Italy), H-1869 and SK-Mes-1 cells in Dulbecco's modified Eagle's Medium (DMEM)/F12 and DMEM (Gibco, Grand Island, NY), respectively, supplemented with 10% heat-inactivated fetal bovine serum (Aurogene) and 1% penicillin/streptomycin mixture and routinely tested to confirm mycoplasma-free status (MycoAlert-Mycoplasma Detection Kit, Lonza, Rockland, ME, USA). All cell lines were maintained at 37°C in a humidified atmosphere with 5% CO2.

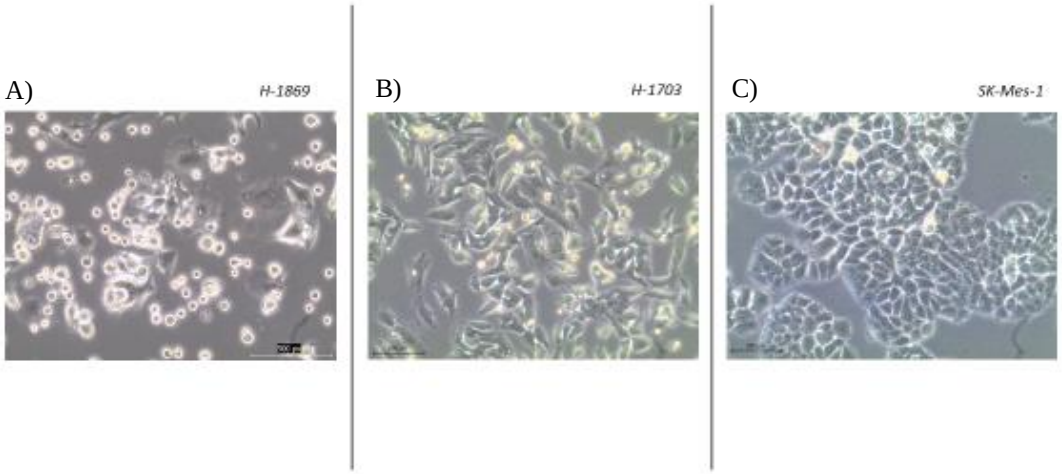

Figure 2.1. Squamous Cell Lung Cancer cell lines.
Photomicrographs of SQLC cell lines which are used in the *in vitro* experiments. A) H-1869, B) H-1703, C) SK-Mes-1. Scale bar, 100 μm.

2.2 Next Generation Sequencing (NGS) Analysis

DNA from SQLC cell lines was obtained by QIAmp AllPrep mini Kit (Qiagen) according to manufacturer protocol and qualified as reported elsewhere [55,56]. A SQLC custom panel targeting selected regions of 36 candidate oncogenes and tumor suppressor genes was designed based on the results of published WGS and exome data [57-59]. The genes included in the panel are: *AKT1*, *APC*, *BCL2L1*, *CCND1*, *CCND2*, *CDKN2A*, *CDKN2B*, *DDR2*, *EGFR*, *ERBB2*, *FGFR1*, *FGFR2*, *FGFR3*, *FRS2*, *KIT*, *MDM2*, *MET*, *MYC*, *MYCL*, *MYCN*, *NFE2L2*, *NOTCH1*, *PDGFRA*, *PIK3CA*, *PTEN*, *RB1*, *RICTOR*, *SMAD4*, *SOX2*, *TERT*, *TET2*, *TIAF1*,

TP53, TP63, TSC2 and *TUBG1*. Twenty nanograms of DNA were used for multiplex PCR amplification. The quality of the obtained libraries was evaluated by the Agilent 2100 Bioanalyzer on-chip electrophoresis (Agilent Technologies). Emulsion PCR to construct the libraries of clonal sequences was performed with the Ion OneTouch™ OT2 System (Life Technologies). Sequencing was run on the Ion Proton (PI, Life Technologies) loaded with Ion PI Chip v2. Data analysis, including alignment to the hg19 human reference genome and variant calling, was done using the Torrent Suite Software v.5.0 (Life Technologies). Filtered variants were annotated using a custom pipeline based on vcflib (https://github.com/ekg/vcflib), SnpSift [60], the Variant Effect Predictor (VEP) software [61] and NCBI RefSeq database. Additionally, alignments were visually verified with the Integrative Genomics Viewer (IGV) v2.3 [62] to further confirm the presence of mutations identified by exome and targeted sequencing. CNV calling, was done using Ion Reporter v.5.0 and the paired samples workflow to match tumor and normal samples (Thermo Fisher).

2.3 FISH experiments

Fluorescence in Situ Hybridization (FISH) was performed on FFPE samples and cell lines (both metaphases and interphases/nuclei) to measure *Rictor* copy-number variations using commercially available FISH spectrum red probe designed to hybridize on chr:5p13.1, (Empire Genomics, USA) and Centromere 5-control spectrum green probe at chr:5p11, (Empire Genomics, USA). The telomeric probes 5p (spectrum green) and 5q (spectrum red) were purchased from Vysis/Abbott

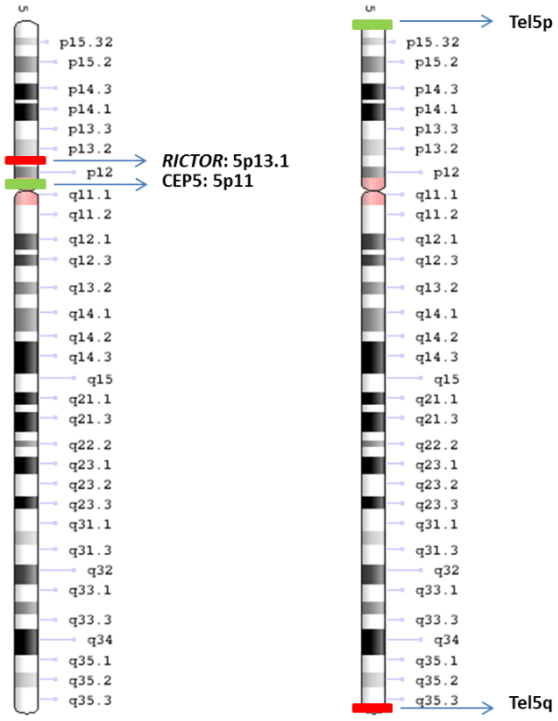

Figure 2. 2. FISH probes targeting the chromosome 5. Left) Rictor probe (red) and Cep5 probe (green) on chromosome 5. Right) Telomeric 5p (green) and telomeric 5q (red) probes.

Molecular. Briefly, 3 µm thick sections from tissue microarray were mounted on positively charged slides and air dried. FFPE sections were deparaffinized with two 10-min washes in xylene, hydrated in 100%, 85%, and 70% ethanol solutions with this order for 10 min each, rinsed in distilled water for 10 min, fixed in methanol:acetic acid 3:1 v/v for 10 min and air dried. Next, the sections were treated in a 2XSSC solution for 15 min at 37^{o}C, and then dehydrated in consecutive 70%, 85%, and 100% ethanol solutions for 1 min each, then dried. The sections were then bathed in 0.1 mM citrate buffer (pH 6) solution at 85^{o}C for 30 min and again dehydrated in a series of ethanol solutions and dried. The slides were incubated in 0.75 ml of pepsin (Sigma) solution (4 mg/ml in 0.9% NaCl, pH 1.5) for 10 min at 37°C, washed again, dehydrated again in graded ethanol solutions (70%, 85%, and 100%) for 2 min each and dried. A total of 10 µl *Rictor* probe was placed on the designated hybridization area and sealed with rubber cement. A ThermoBrite denaturation-hybridization system (Abbott Molecular) set at 80°C was used for co-denaturation of probe and target DNA for 10 min, before hybridization at 37°C overnight. The rubber cement and coverslip were removed, and the slides were placed in 0.3% NP-40/2X saline-sodium citrate (SCC) solution at first for 15 min, at room temperature (RT) and then at 72°C for 2 min. The sections were then rinsed in H_2O for 1 min, air dried, and counterstained with 10 µl of nuclear stain 4',6-diamidino-2-phenylindole (DAPI) II /Antifade (ProLong Gold Antifade Reagent with DAPI; Life Technologies). Cell cultures were treated with colcemid (Gibco KaryoMax Colcemid solution in PBS, LifeTechnologies) at a final concentration of 10ng/mL for 16 hours (overnight) at

37°C and metaphases harvest was carried out according to standard protocols. Briefly, PBS washed cells were treated with hypotonic solution (0.075 M KCl for 15 min at RT) and fixed in methanol/acetic acid 3:1 v/v. Air dried metaphase spreads and nuclei spreads slides were analyzed by FISH for *Rictor* copy number following standard procedures. The slides were examined using an Olympus BIX-61 microscope (Olympus, Hamburg, Germany) with appropriate fluorescence excitation/emission filters. The signals were recorded by a CCD camera (Olympus Digital Camera). For microscopic evaluation, at least 100 intact and non-overlapping cell nuclei and 25 metaphases were scored for *Rictor* and Centromere 5 copy-number variations. A *Rictor*/chromosome 5 ratio of 2.0 or higher represents gene amplification, while the presence of more than 4 *Rictor* gene copies without gene amplification is defined as *Rictor* polysomy.

2.4 RNA extraction and real-time PCR

SQLC cells at approximately 70% of confluency were washed with PBS and collected in 1ml of TRIZOL reagent using a cell scraper and then the solution stored at -80^{o}C. RNA was extracted after following phenol-chloroform protocol and quantified by using the NanoDrop 2000 Spectrophotometer. 1μg of extracted RNA was reverse-transcribed into cDNA by using high capacity cDNA reverse transcription kit (Life technologies). The *Rictor* TaqMan gene expression assay (Assay ID: Hs00380903_m1) was used following the manufacturer's instructions. mRNA expression was quantified using the ΔΔCt method and housekeeping gene, human *HPRT1*, was used as endogenous control.

2.5 Western Blotting and antibodies

Total protein from cell lines was extracted by adding Cell Lysis buffer 1X (Cell signaling Technology) including protease and phosphatase inhibitor and maintaining on ice for at least 1 hour, followed by centrifugation for 15 min, 14.000 g 4^{o}C. Protein concentration was determined by bicinchoninic acid protein assay (QuantumProtein, Euroclone). Protein samples of equal amount (30μg) were loaded onto NuPAGE^{TM} 4-12% Bis-Tris Gel (Thermo Scientific), electrophoresed and transferred to a PVDF membrane (Thermo Scientific). The membrane was blocked

in 5% nonfat dried milk for 1 hour at room temperature and probed with primary antibodies in dilutions according manufacturer's recommendations, against phospho-mTOR Ser2448 (#2976), Rictor (abcam ab70374), phospho-Rictor (#3806), Akt (#9272), phosphor-Akt(S473) (#4060), phospho-S6 (#4857), phospho-4E-BP1 (#2855), Hsp90 (#4877), for overnight incubation at 4^{o}C. Apart Rictor, the rest antibodies were purchased from Cell Signaling Technology. The immunoreactive bands were detected with enhanced chemiluminescence ECL reagents (GE Healthcare BioSciences Corp).

2.6 Cell viability assays

Cells were seeded in 96-well (4.000/10.000/18.000 cells per well for H-1703/H-1869/SK-Mes-1) or in 6-well plate (40.000/190.000 cells per well for H-1703/SK-Mes-1), for short- (3 days) and long-term (7 days) treatment, respectively. Twenty-four hours after seeding, serial dilutions of drugs were added to the media and cell viability measured after 3 or 7 days by Crystal violet assay. DMSO-only (maximum concentration of 0.1%) treated cells were considered as controls. In case of long-term treatments, drug-containing media were refreshed after three days. Small molecule inhibitors AZD2014 (mTORC1/2) and PF-05212384 (PI3K/mTOR) were obtained from Selleckchem (Houston, TX, USA). All drugs were used as monotherapy. Each experiment was performed in triplicate.

2.7 Rictor silencing

H-1703 and H-1869 cells were sub-cultured appropriately and placed in 6-well plate in order to obtain a 50-60% confluent cell culture 24 hours before transfection. Three different SMARTvector Doxycycline-Inducible Lentiviral *Rictor* targeting shRNAs and one scramble shRNA (Dharmacon, GE *Dharmacon*, Pitssburgh, PA, USA) as negative control were transfected according the manufacturer's protocol.
Set of 3 SMARTvector Human Inducible shRNA:

- V3SH7669-228720130, Mature Antisense: ATATGTAGCAGCGTATTAC
- V3SH7669-229062802, Mature Antisense: CAAAATTAGCACCTCACTC
- V3SH7669-230704057, Mature Antisense: CTCGGAGATACTGATCCCG

Polybrene (Millipore™) 10 μg/mL was also used to increase the efficiency of transfection. Transfected cells were then treated with puromycin, as selection antibiotic, for isolation of successfully transfected clones. After evaluation of *Rictor* levels by qPRC and immunoblotting, the most efficient shRNA was selected for transfecting the other cell lines.

3 Results

3.1 Genetic landscape of SQLC cell lines

To characterize the *in vitro* models, we performed high coverage sequencing of three SQLC cell lines targeting known oncogenes and tumor suppressor genes. Sequencing data were used to identify single nucleotide variations, small indels, and gene copy-number variations. Results are summarized in **Table 3.1**. Notably, we found that all cell lines had gains of *Rictor*. This is in line with previous observations.

	H-1869	H-1703	SK-Mes-1
EGFR	WT	WT	Amplification
TSC1/C2	WT	WT	WT
PTEN	WT	WT	LOH
PI3K	WT	WT	WT
RICTOR	Amplification (8 copies)	Amplification (4 copies)	Amplification (3 copies)
Akt	WT	WT	WT
FGFR1	WT	Amplification	WT
PDGFRa	WT	Amplification	WT
KRAS	WT	WT	WT

Table 3.1. NGS analysis of 3 SQLC cell lines for a set of selected cancer-related genes.

Moreover, FGFR1 amplification (a frequent finding in SQLC) was detected in H-1703, while EGFR amplification and PTEN loss were identified in SK-Mes-1.

To orthogonally validate presumed *Rictor* amplification, we performed both metaphase and interphase FISH analysis on the 3 SQLC cell lines. A high number of copies for both *Rictor* and CEP5 were detected for all cell lines, although with a *Rictor*/CEP5 ratio of 1 **(Fig. 3.1)**. Therefore, we hypothesized that the gain of *Rictor* detected through sequencing is likely due to polysomy of the short arm of chromosome 5 (5p) rather than to focal amplification-as suggested by a previous study [47].

Indeed, when using a telomeric 5q probe combined with telomeric 5p probe in H-1703 we could observe an unbalance between the two signals with many more signals for 5p **(Fig. 3.2)**. In keeping with 5p polysomy, other genes (e.g., TERT,

SDHA) located on the short arm of chromosome 5 were affected by gain in our cell lines. Despite that gene amplification is not the responsible mechanism, differences in terms of copy number of *Rictor* among cell lines were reported. H-1869 harbors the highest number with 10 *Rictor* copies followed by H-1703 with 6 and then SK-Mes-1 with 4 *Rictor* copies.

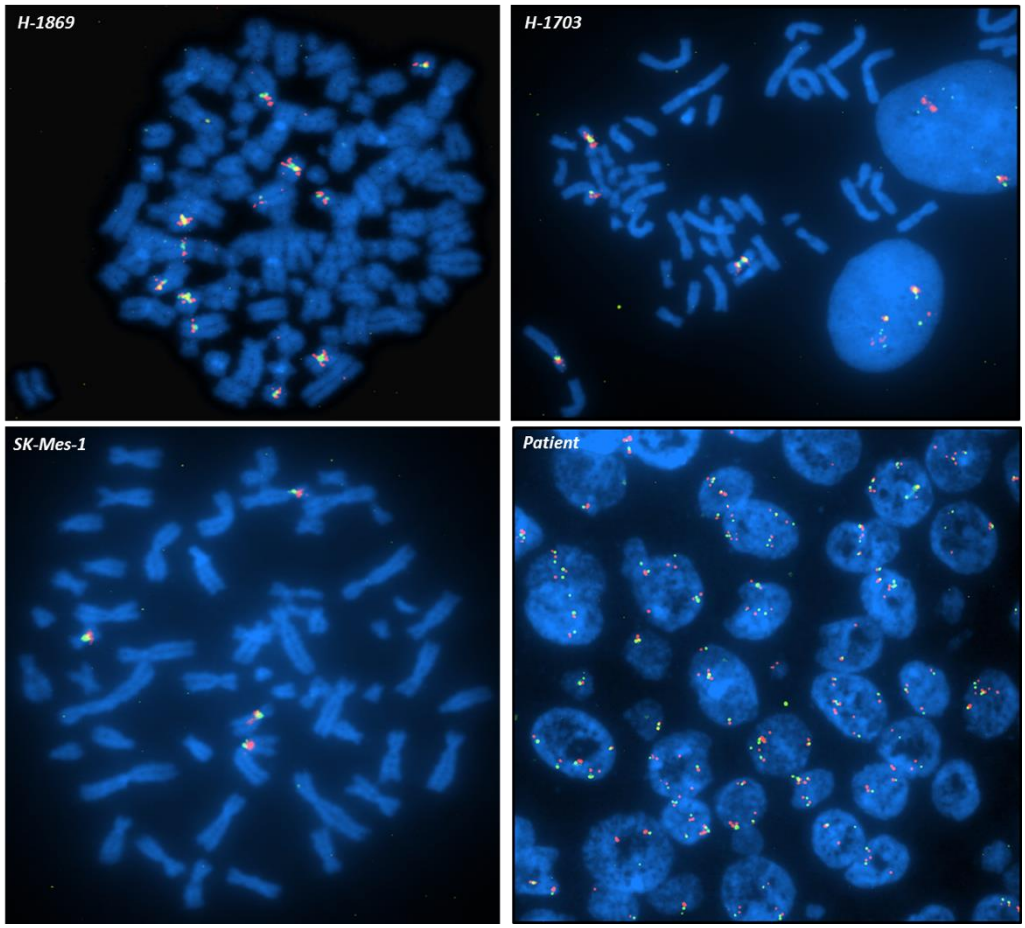

Figure 3.1. Identification of Rictor copy gain by FISH testing in SQLC cell lines and patient samples.

Representative metaphase and interphase FISH images. All three cell lines and patient sample present >2 for both *Rictor* (red) and Cep 5 (green) signals, producing a ratio approximately 1.

Next, we sought to confirm the results in some SQLC patients belonging to our cohort (n=60) we use for different analyses also in other projects. The use of the two different probes (centromeric and telomeric) for normalization of locus-specific signals confirmed that in SQCL 5p polysomy, rather than focal gene amplification,

explains the high number of *Rictor* copies detected at targeted sequencing by us and other groups **(Fig. 3.1 and 3.2)**.

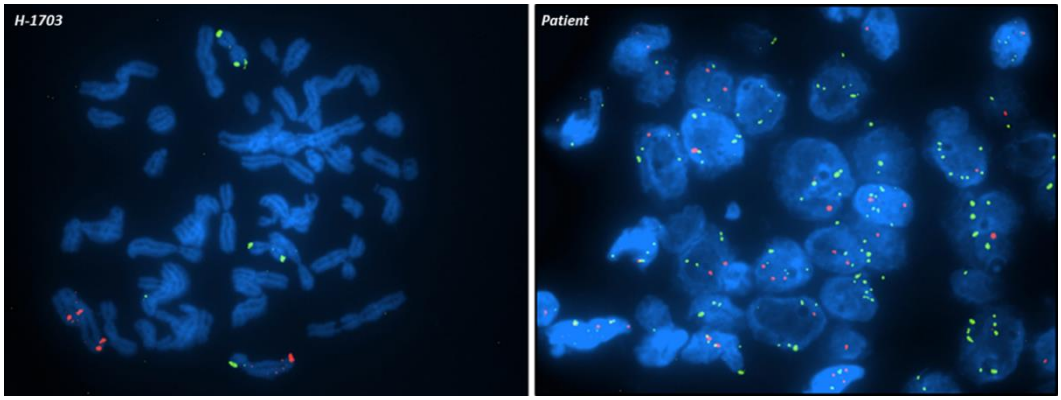

Figure 3.2. FISH experiments probing with telomeric probes of chromosome 5 in H-1703 and SQLC patient sample.

Representative metaphase and interphase FISH images of SQLC cell line and patient sample with tel 5q (red) and tel 5p (green) probes. Both H-1703 and patient sample present a large imbalance of signals with many more for the 5p probe.

3.2 Rictor and PI3K/mTOR pathway flux

We sought to assess whether and how differences in *Rictor* gene dosage affected: i) *Rictor* mRNA transcript levels and ii) PI3K/mTOR pathway's flux in SQLC cell lines. qRT-PCR analysis of the 3 cell lines revealed that mRNA transcripts encoding for *Rictor* are more abundant (7-fold increase) in H-1869 as compared to H-1703 and SK-Mes-1 **(Fig. 3.3)**. Analysis of whole protein lysates from the 3 cell lines confirmed the qPCR data; the H-1869 cell line showed the highest abundance of Rictor (**Figure 3.4**). Unexpectedly, the level of Rictor did not parallel those of phospho-Akt (S473), a well-established marker of PI3K/mTOR pathway activation, suggesting that in our preclinical models there is no correlation between Rictor level and activation of the PI3K/mTOR pathway (**Figure 3.4**).

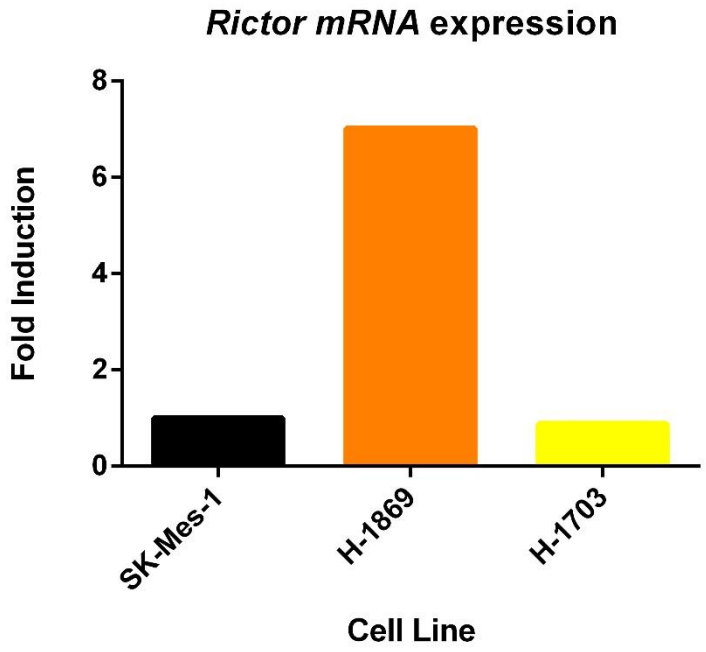

Figure 3.3. Expression levels of mRNA transcripts for Rictor.
Quantitative real time PCR of Rictor mRNA in SQLC cell lines. The graph represents fold change of mean expression relative to SK-MES-1 (cell line with less Rictor copies), given a value of 1.

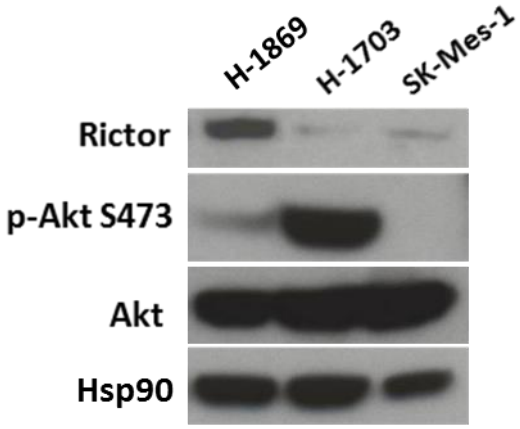

Figure 3.4. Rictor levels and PI3K/Akt pathway activation in SQLC cell lines.
Immunoblotting of whole protein lysate from H-1703 SK-Mes-1, and H-1869 probed with antibodies regarding mTOR pathway.

3.3 Pharmacological inhibition of PI3K/mTOR signaling pathway in SQLC cell lines

In order to verify whether a causative link among *Rictor* gene dosage/transcript/protein and sensitivity to pathway inhibitors exists, we treated the

3 SQLC cell lines with 2 different PI3K/mTOR targeted inhibitors. First, we challenged the 3 cell lines with the dual mTORC1/2 inhibitor AZD2014 continuously for 3 and 7 days. H-1703 and SK-Mes-1 showed similar responses to 3 days of treatment **(Fig. 3.5 A)**, while H-1703 was more sensitive to the prolonged exposure to the drug **(Fig. 3.5 B)**. H-1869 cell line, which shows the highest levels of Rictor at both mRNA and protein levels, was poorly responsive to both 3 and 7 days of continuous treatment **(Figure 3.5 A and B)**.

More evident differences were observed when cell lines were challenged with a dual PI3K/mTOR inhibitor (PF-05212384), where H-1703 was much more sensitive than SK-Mes-1 and H-1869 both in short- and long-term **(Fig. 3.5 C and D)**. Intriguingly and against our initial hypothesis, H-1869 did not look sensitive to PI3K/mTOR inhibition regardless the targeted inhibitor. Collectively, H-1703 which presents, based on the immunoblotting experiments, the higher PI3K/mTOR pathway activity is the cell line that respond more efficiently to the targeted inhibition. In contrast, the higher *Rictor* genetic/transcript/protein profile that H-1869 harbors did not affect drug efficacy. In conclusion, *Rictor* dosage does not predict sensitivity to PI3K/mTOR inhibitors *in vitro*.

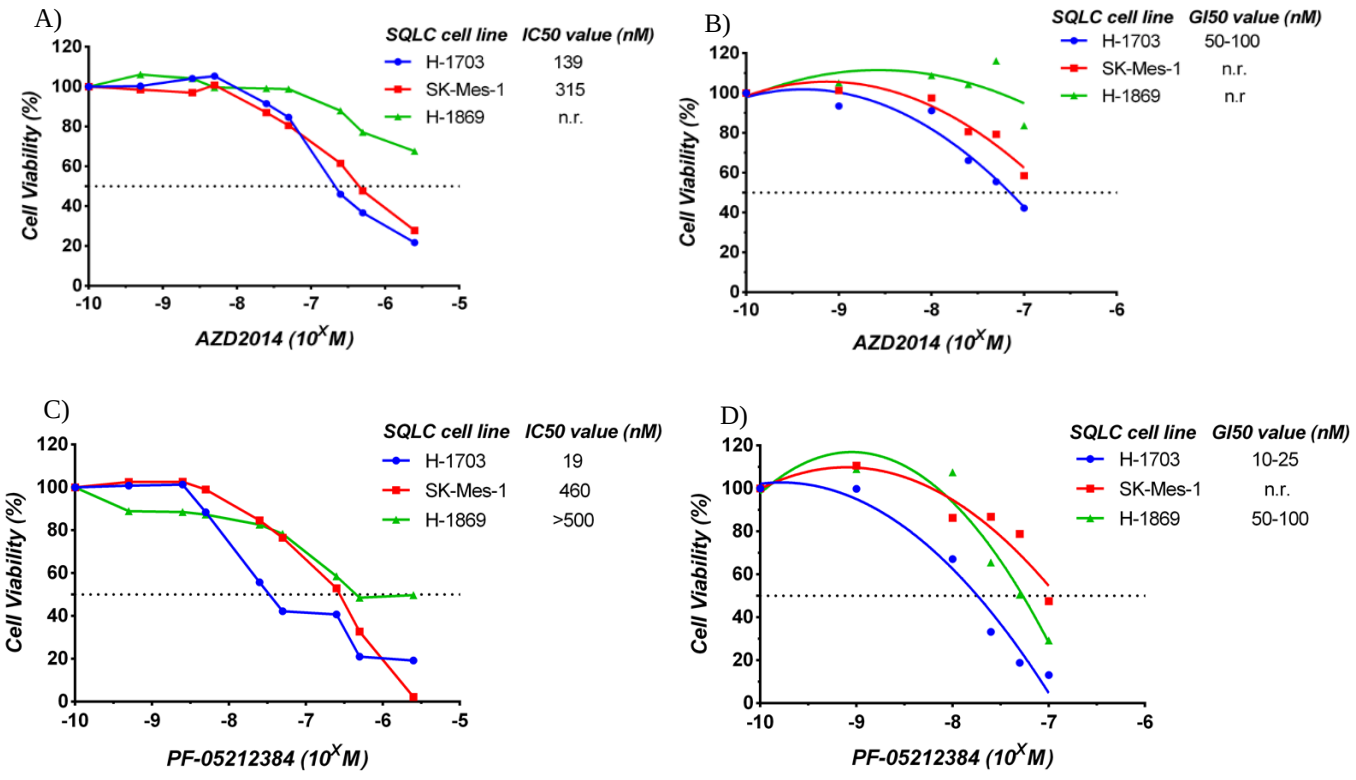

Figure 3.5. SQLC cells lines treated with PI3K/mTOR targeted inhibitors. A) Short-term (3 days) treatment with AZD2014. B) Long-term (7 days) treatment with AZD2014, C) Short-term (3 days) treatment with PF-05212384, D) Long-term (7 days) treatment of cell lines with PF-05212384. Cell viability assays were conducted by treating SQLC cells with increasing concentrations of drugs. The effect on cell viability was measured with crystal violet assay. The plates were read at 595 nM using a microplate reader and results are reported as percent of control.

3.4 Pharmacologic treatment blocks signaling axis downstream of mTORC1 and mTORC2.

Given the observed effects of the drug treatment on cell viability of SQLC cell line, we sought to assess whether the used drugs were actually able to modulate the pathway in preclinical models. Therefore, we treated H-1869, H-1703 and SK-Mes-1 with sub-IC50 concentration of AZD2014 and PF-05212384 for few hours (2 and 4 hours). In H-1703, AZD2014 rapidly reduced phosphorylation of Akt at Serine 473 (2hrs), but without affecting the levels of the activated forms of mTOR or phospho-Rictor, nor those of downstream mTOR targets (S6 and 4EBP1) **(Fig. 3.6 Left)**. After 4 hours of exposure to AZD2014, pathway rewiring was observed in H-1703 as demonstrated by the increased levels of phospho-Akt **(Fig. 3.6 Right)**. Conversely, PF-05212384 induced a rapid and durable reduction in the levels of the phosphorylated forms of Rictor and Akt, without affecting the phosphorylation of mTOR at the Serine 2448. Consistent with a dramatic reduction in the phosphorylation of Rictor and activation of Akt, reduced levels of the phosphorylated forms of S6 were observed in H-1703 exposed to PF-05212384 **(Fig 3.6)**.

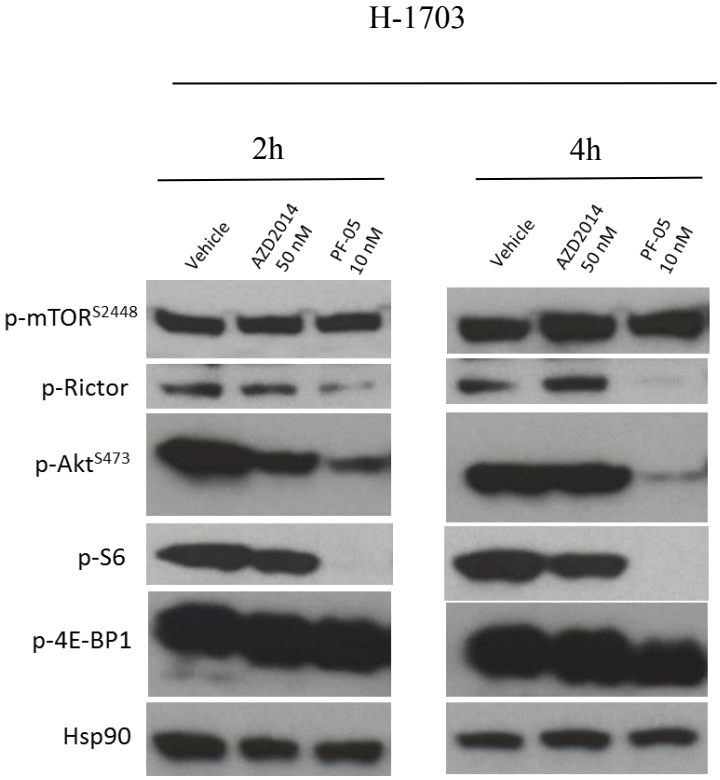

Figure 3.6. Post-treatment immunoblotting of H-1703 for the PI3K/mTOR pathway.
Immunoblotting for components of the PI3K/mTOR pathway components in H-1703 cells, untreated or treated with AZD2014 or PF-05212384 at the concentrations indicated after 2 and 4 hours. Hsp90 was used as loading control

In SK-Mes-1, 2-hour treatment with AZD2014 or PF-05212384 rapidly decreased the phosphorylation levels of Rictor, 4E-BP-1, and p-S6 levels. Phosphorylation levels of mTOR at S2448 were unaffected after 2 hours of treatment. In line with previous observations, SK-Mes-1 did not show detectable level of the phosphorylated Akt at S473 neither baseline nor after 2 hours of treatment pressure **(Fig. 3.7 Left)**.

Following 4 hours of exposure to drugs, the effect on the phosphorylation levels of 4E-BP-1, p-Rictor and p-S6 levels were persistent, and interestingly we could observe a reduction of phospho-mTOR at S2448 **(Fig. 3.7 Right)**.

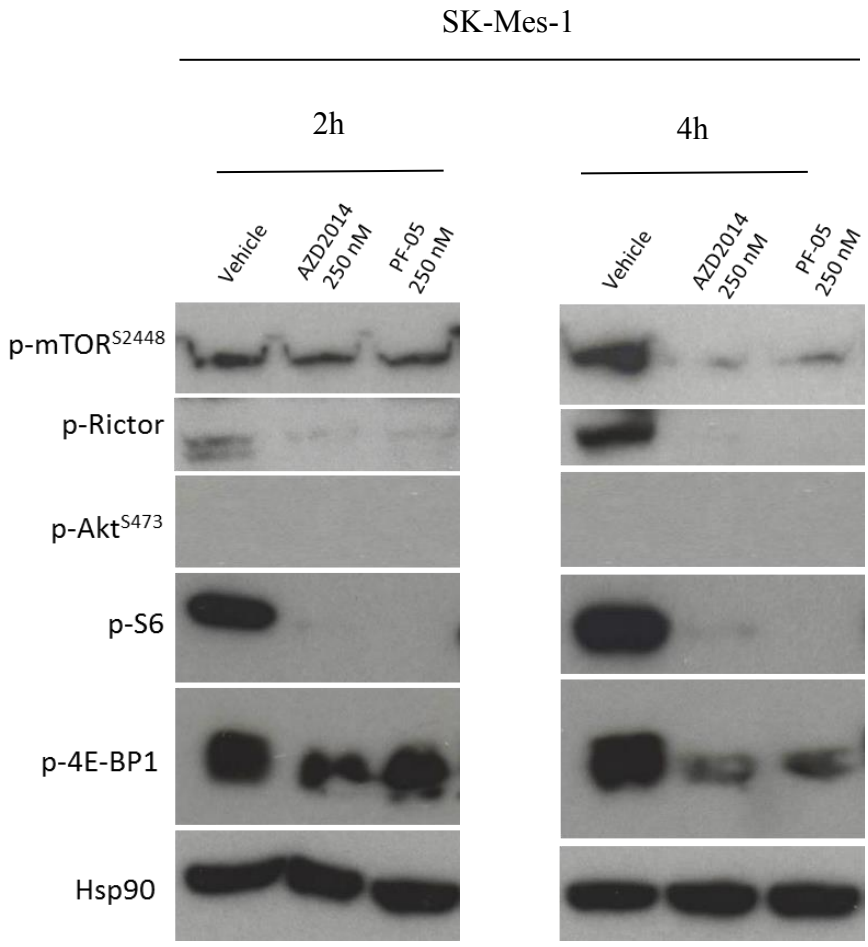

Figure 3.7. Post-treatment immunoblotting of SK-Mes-1 for the PI3K/mTOR pathway. Immunoblotting for related mTOR pathway components in SK-Mes-1 cells, untreated or treated with AZD2014 or PF-05212384 at the concentrations indicated after 2 and 4 hours. Hsp90 was used as internal control

In H-1869, 2 hours of AZD2014 (dual mTORC1/2 inhibitor) treatment lead to an increase in the levels of both p-mTOR and p-S6, despite a slight reduction in the level of p-Rictor **(Figure 3.8)**. Levels of the activated form of Akt were largely unaffected **(Figure 3.8)**. Two hours of treatment with the dual PI3K/mTOR inhibitor PF-05212384 caused a marked reduction in the level of the activated form of Rictor, while increasing levels of p-mTOR and p-S6. Collectively, these data suggest that targeting of the PI3K/mTOR pathway in cells with high levels of Rictor has paradoxical effect in the activation of mTOR and some of its downstream component, namely S6 Kinase. These results might partially explain why the targeted agents were largely ineffective in reducing viability of H-1869.

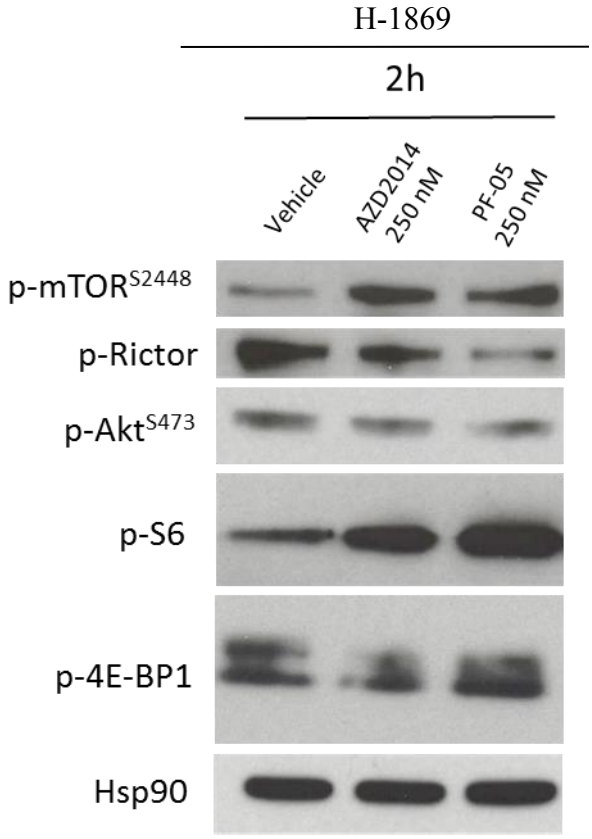

Figure 3.8. Post-treatment immunoblotting of H-1869 for the PI3K/mTOR pathway. Immunoblotting for related mTOR pathway components in H-1869 cells, untreated or treated with AZD2014 or PF-05212384 at the concentrations indicated after 2. Hsp90 was used as internal control

3.5 Genetic perturbation of *Rictor* does not affect sensitivity of SQLC cell lines to targeted inhibitors

Although the previous experiments showed that Rictor is not predictive of response to PI3K/mTOR inhibition, we attempted at exploring this finding also through genetic shRNA perturbation. To achieve this, we used a doxycycline inducible shRNA system. First, we screened the three shRNAs and identified the most effective, which was able to reduce Rictor levels by 70% in H-1703 (**Figure 3.9 A and 3.9 B**)

Accordingly, reduction of Rictor associated with reduction of activation through the pathway as measured by reduced levels of p-Akt S473, while not affecting phosphorylation of two different key residues of mTOR (**Fig. 3.9 A**). Challenging

the transfected cells with our most effective drug compound, PF-0521238, we did not observe differences regarding IC50 between *R*ictor proficient (scramble shRNA) and *Rictor* deficient cells **(Fig. 3.9 C)**.

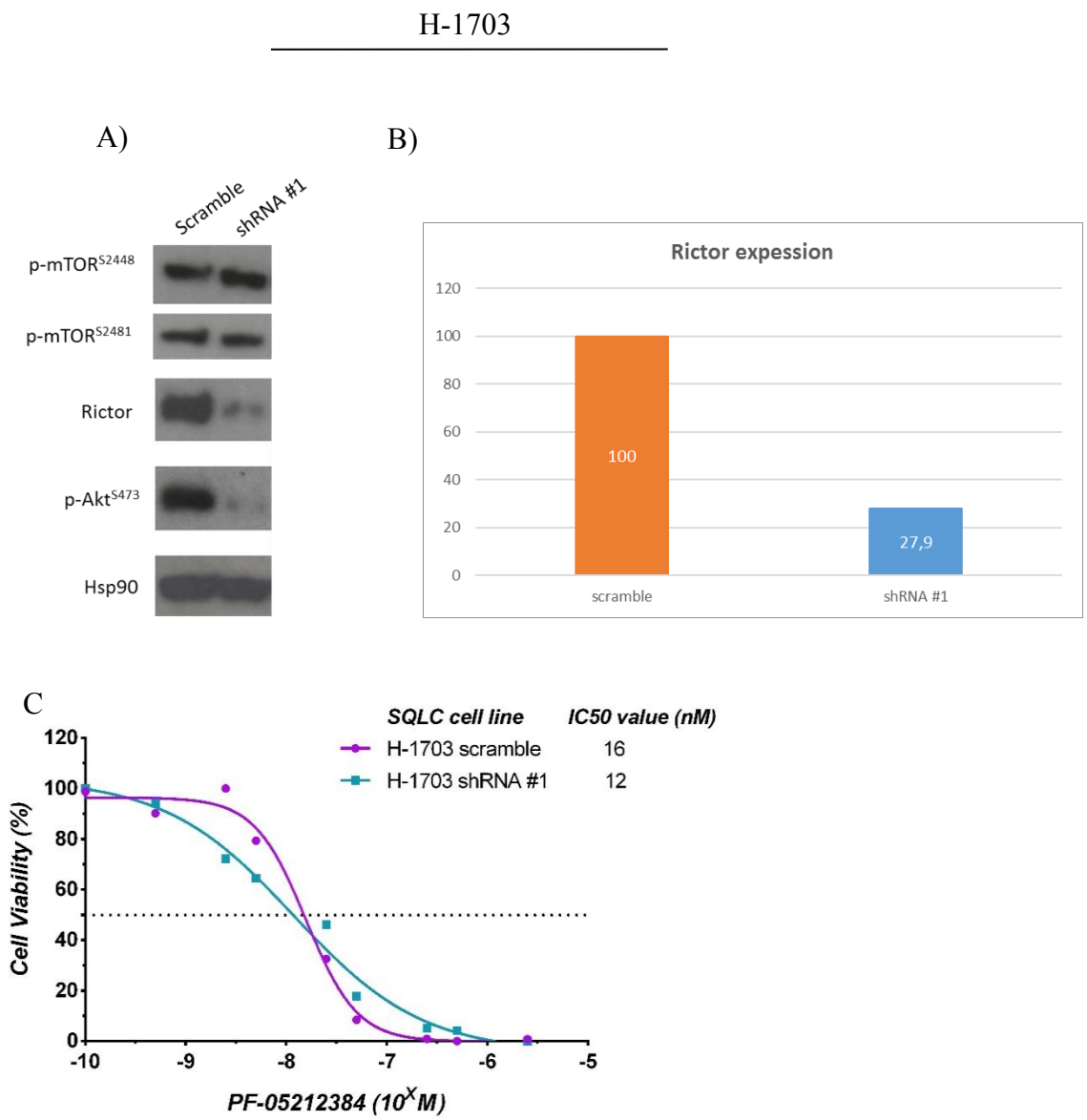

Figure 3.9. Rictor silencing in H-1703 does not affect the drug sensitivity to PI3K/mTOR inhibition.

A) Western Blot confirming efficient Rictor knockdown in H-1703. B) Quantification of Rictor protein expression after induction of the shRNAs with 100 ng/ml of doxycycline. Protein expression was quantified by ImageJ software. C) Graph showing cell viability assay in H-1703 transfected with scramble and targeting shRNA.

We also performed genetic deletion of *Rictor* also in the H-1869, the cell line harboring the highest number of *Rictor* copies, even if appeared to be the most

resistant compared to other two SQLC cell lines. Reduction of Rictor levels by the shRNAs in H-1869 was less efficient (around 50%) as compared to H-1703 (**Fig. 3.10 A and B**).

However, no differences in terms of drug sensitivity were observed between *Rictor* proficient and *Rictor* deficient cells after treatment with either AZD2014 or PF-05212384 **(Fig. 3.10 C)**.

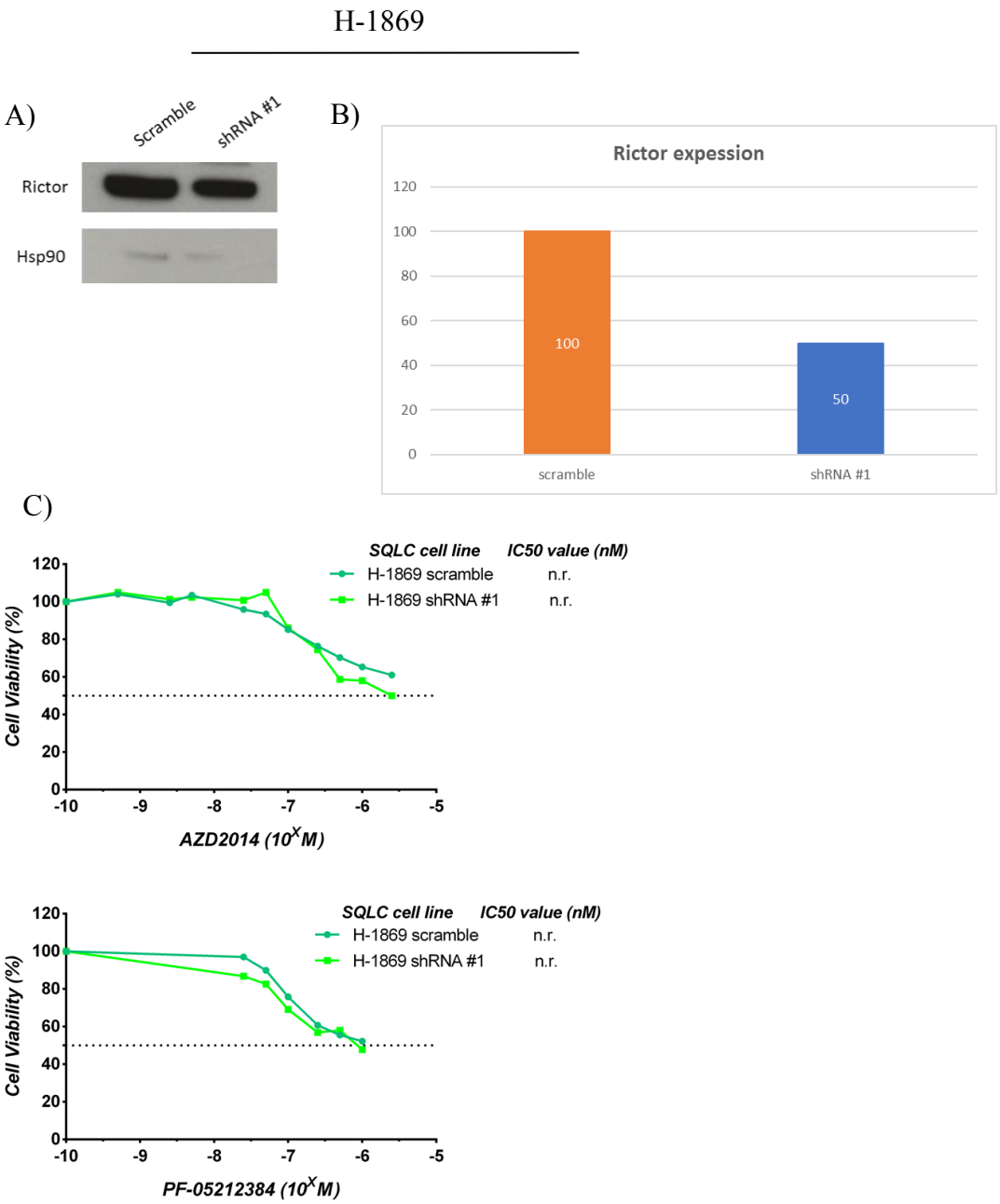

Figure 3.10. Rictor silencing in H-1703 does not affect the drug sensitivity to PI3K/mTOR inhibition.

A) Western Blot confirming Rictor knockdown in H-1869, B) Quantification or Rictor protein expression following induction of the targeting shRNA with 250-500 ng/ml of doxycycline. Protein expression was quantified by ImageJ software, C) graphs showing cell viability assays in H-1869 transfected with scramble and targeting shRNA.

4 Discussion

Lung cancer is a deadly disease lacking life-extending treatments for the vast majority of patients. However, the advent of TKIs after the identification of EGFR mutations in LUAD patients was not only a major breakthrough in lung cancer treatment but also paved the way for a pioneer, biomarker-based research strategy. Towards this, extensive studies explored SQLC genomic status unrevealing several signatures of genomic alterations. Several components of the FGFR and PI3K/mTOR pathways were most frequently affected by genetic alterations in SQLC patients. However, their involvement in SQLC onset and progression is poorly understood to date, and clinical trials aimed at inhibiting different effectors of the aforementioned signaling pathways generated mediocre results. The poor translation of findings from comprehensive genetic analyses to the clinical setting is also contributed by the fact that correlative rather than causative relationships has been established for the majority of genetic alterations in SQLC. In 2015, *Cheng et al*. reported of *Rictor* amplification in SQLC and, using an individual cell line (H-1703), they suggested an oncogenic and predictive role for Rictor [47]. Building on this, we sought to assess whether or not Rictor is a true dependency in subsets of SQLC and, more importantly, whether it represents a valid predictive biomarker. First, we demonstrated that *Rictor* is not amplified in SQLC and that copy-number gains, as assessed by NGS, are rather due to polysomy of 5p and not a focal gene amplification. The same results were also observed *in vivo*, by performing FISH analyses on patients' tissue. Our data are in disagreement with those reported by *Cheng et al.*, and this is due to different experimental procedures used to identify and validate *Rictor* copy-gains. Indeed, *Cheng et al*. reported focal *Rictor* amplification in a subset of SQLC patients based on DNA targeted sequencing [47]. Similarly, our targeted DNA sequencing data also suggested *Rictor* amplification, albeit we noticed that other genes lying on the same chromosomal arm were called as amplified (*IL7R*, *FGF10*, *PTGER4*). To validate the NGS finding, we have chosen a more comprehensive FISH approach as compared to that used by *Cheng and colleagues* [47], as it was based on the use of multiple probes to normalize the signal of the *Rictor*-specific probe. In line with a polysomy of the short arm of chromosome 5, no amplification was identified in either cell lines or tissues when

locus specific signals were normalized using centromeric or telomeric probes on the 5p. Similar to the results obtained by *Cheng et al*. [47], we mistakenly assigned amplification when using 5q telomeric probes. In agreement with our observation, Sakre et al. performed targeted exome sequencing in SCLC and reported amplification of *Rictor*, *FGF10* and *IL7R*, all neighboring genes located on 5p13. Intriguingly, targeted genes on 5q arm were not amplified. Therefore, we can confidently conclude that there is no recurrent focal amplification of *Rictor* in SQLC but rather polysomy of 5p, which could lead to increase gene dosage. Therefore, here we tested whether high dosage of *Rictor* could be a driver of disease and a potential therapeutic target in subset of SQLC. We screened 3 different SQLC cell lines and found that, despite different genetic background, all harbored CNG but with different levels. As expected, high CNG of *Rictor* corresponded to increased mRNA and protein expression. Unexpectedly, high levels of Rictor did not correspond to increased fluxes through the PI3K/mTOR pathway as assessed by the levels of the phospho-activated form of Akt (S473). Consistent with the results of the pathway analysis, the SQLC cell line (H-1869) harboring highest level of *Rictor* showed poor sensitivity towards 2 effective multitarget compounds (AZD2014 and PF-05212384) of the PI3K/mTOR pathways. In keeping with available literature, levels of p-AKT S473 were instead predictive of sensitivity towards compounds targeting PI3K/mTOR in H-1703 cell line. Indeed, we detected a rapid decrease of p-Akt S473 for H-1703 which can explain the high sensitivity to PI3K/mTOR inhibition. As was anticipated, our drug compounds, effectively modulated the PI3K/mTOR pathway, explaining, at least partially, cancer cell survival impairment which we observed in our cell viability assays. In H-1703, treatment with PF-05212384 modulated stronger and faster the PI3K/mTOR pathway compared to AZD2014 downregulating rapidly p-Akt S473 and p-S6. Indeed, IC-50 values for PF-05212384 and AZD2014 were 19 nM and 139 nM, respectively. Peculiarly, levels of p-mTOR S2448 are not affected by the drugs. Treatment of SK-Mes-1 with the same inhibitors for the same period of time induced an immediate downregulation of p-S6 and p-4E-BP-1. However, total absence of p-Akt S473 expression might render these cells more resistant to the drugs as IC-50 values show, 315 nM and 460 nM for AZD2014 and PF-05212384,

respectively. H-1869 showed only slight decrease of p-Akt S473 and in combination with upregulation of p-S6, the high resistance to the drugs can be explained. Interestingly, p-Rictor is downregulated rapidly and in parallel with p-S6 in H-1703 and SK-Mes-1 cell lines, indicating that a Rictor-specific crosstalk between mTORC1 and mTORC2 might exist. However, in H-1869, the opposite effect is observed. Nevertheless, the exact impact of Rictor phosphorylation on mTORC2 activity is not clear yet.

Finally, we used an inducible system to silence Rictor in SQLC cell lines with different CNG levels. Overall, our data suggest that copy-gain of *Rictor* is not a dependency in SQLC cell lines and does not influence resistance/sensitivity to drug treatments. Following efficient knock down of Rictor, we could successfully modulate pathway fluxes with reduced levels of p-AKT on S473; yet, *Rictor* proficient and deficient cell lines did not show differences in terms of cell viability and sensitivity towards targeted agents.

Collectively, our results suggest that a careful dissection of the role and relevance of candidate should be undertaken using orthogonal approaches before nominating potential therapeutic targets in cancer.

There are multiple examples of genomic aberrations mistakenly proposed as valid therapeutic or prognostic targets in cancer. Correlation is not causation, and a careful dissection of the role of genetic alterations in a given tumor type is mandatory to avoid that experimental efforts (and financial investments) are made towards targeting dispensable genes. Our data strongly suggest that Rictor is not a dependency in SQLC and, further, does not represent a predictive biomarker of response to PI3K/mTOR-targeted therapy. This might suggest that other components of the genetic background of the cell lines might affect sensitivity/resistance towards those compounds.

Nonetheless, genomic aberrations of *Rictor* might affect other cellular behaviors, including invasive capabilities and interaction with the microenvironment. We have now defined a suitable platform of mTORC2 for interrogation of relevant biological questions in SQLC regarding this relatively unexplored signaling entity.

5 Bibliography

1. Malhotra, J.; Malvezzi, M.; Negri, E.; La Vecchia, C.; Boffetta, P. Risk factors for lung cancer worldwide. *Eur Respir J* **2016**, *48*, 889-902, doi:10.1183/13993003.00359-2016.
2. Barta, J.A.; Powell, C.A.; Wisnivesky, J.P. Global Epidemiology of Lung Cancer. *Ann Glob Health* **2019**, *85*, doi:10.5334/aogh.2419.
3. Travis, W.D.; Brambilla, E.; Nicholson, A.G.; Yatabe, Y.; Austin, J.H.M.; Beasley, M.B.; Chirieac, L.R.; Dacic, S.; Duhig, E.; Flieder, D.B., et al. The 2015 World Health Organization Classification of Lung Tumors: Impact of Genetic, Clinical and Radiologic Advances Since the 2004 Classification. *J Thorac Oncol* **2015**, *10*, 1243-1260, doi:10.1097/JTO.0000000000000630.
4. Siegel, R.L.; Miller, K.D.; Jemal, A. Cancer statistics, 2020. *CA Cancer J Clin* **2020**, *70*, 7-30, doi:10.3322/caac.21590.
5. Sutherland, K.D.; Berns, A. Cell of origin of lung cancer. *Mol Oncol* **2010**, *4*, 397-403, doi:10.1016/j.molonc.2010.05.002.
6. Suarez, E.; Knollmann-Ritschel, B.E.C. Squamous Cell Carcinoma of the Lung. *Acad Pathol* **2017**, *4*, 2374289517705950, doi:10.1177/2374289517705950.
7. Ma, Y.; Fan, M.; Dai, L.; Kang, X.; Liu, Y.; Sun, Y.; Xiong, H.; Liang, Z.; Yan, W.; Chen, K. Expression of p63 and CK5/6 in early-stage lung squamous cell carcinoma is not only an early diagnostic indicator but also correlates with a good prognosis. *Thorac Cancer* **2015**, *6*, 288-295, doi:10.1111/1759-7714.12181.
8. Affandi, K.A.; Tizen, N.M.S.; Mustangin, M.; Zin, R. p40 Immunohistochemistry Is an Excellent Marker in Primary Lung Squamous Cell Carcinoma. *J Pathol Transl Med* **2018**, *52*, 283-289, doi:10.4132/jptm.2018.08.14.
9. Perez-Moreno, P.; Brambilla, E.; Thomas, R.; Soria, J.C. Squamous cell carcinoma of the lung: molecular subtypes and therapeutic opportunities. *Clin Cancer Res* **2012**, *18*, 2443-2451, doi:10.1158/1078-0432.CCR-11-2370.
10. Stewart, P.A.; Welsh, E.A.; Slebos, R.J.C.; Fang, B.; Izumi, V.; Chambers, M.; Zhang, G.; Cen, L.; Pettersson, F.; Zhang, Y., et al. Proteogenomic landscape of squamous cell lung cancer. *Nat Commun* **2019**, *10*, 3578, doi:10.1038/s41467-019-11452-x.
11. Takeda, M.; Nakagawa, K. First- and Second-Generation EGFR-TKIs Are All Replaced to Osimertinib in Chemo-Naive EGFR Mutation-Positive Non-Small Cell Lung Cancer? *Int J Mol Sci* **2019**, *20*, doi:10.3390/ijms20010146.
12. Reck, M.; Rodriguez-Abreu, D.; Robinson, A.G.; Hui, R.; Csoszi, T.; Fulop, A.; Gottfried, M.; Peled, N.; Tafreshi, A.; Cuffe, S., et al. Updated Analysis of KEYNOTE-024: Pembrolizumab Versus Platinum-Based Chemotherapy for Advanced Non-Small-Cell Lung Cancer With PD-L1 Tumor Proportion Score of 50% or Greater. *J Clin Oncol* **2019**, *37*, 537-546, doi:10.1200/JCO.18.00149.
13. Carbone, D.P.; Reck, M.; Paz-Ares, L.; Creelan, B.; Horn, L.; Steins, M.; Felip, E.; van den Heuvel, M.M.; Ciuleanu, T.E.; Badin, F., et al. First-Line Nivolumab in Stage IV or Recurrent Non-Small-Cell Lung Cancer. *N Engl J Med* **2017**, *376*, 2415-2426, doi:10.1056/NEJMoa1613493.
14. Cancer Genome Atlas Research, N. Comprehensive genomic characterization of squamous cell lung cancers. *Nature* **2012**, *489*, 519-525, doi:10.1038/nature11404.
15. Mantripragada, K.; Khurshid, H. Targeting genomic alterations in squamous cell lung cancer. *Front Oncol* **2013**, *3*, 195, doi:10.3389/fonc.2013.00195.
16. Paik, P.K.; Pillai, R.N.; Lathan, C.S.; Velasco, S.A.; Papadimitrakopoulou, V. New Treatment Options in Advanced Squamous Cell Lung Cancer. *Am Soc Clin Oncol Educ Book* **2019**, *39*, e198-e206, doi:10.1200/EDBK_237829.

17. Govindan, R.; Ding, L.; Griffith, M.; Subramanian, J.; Dees, N.D.; Kanchi, K.L.; Maher, C.A.; Fulton, R.; Fulton, L.; Wallis, J., et al. Genomic landscape of non-small cell lung cancer in smokers and never-smokers. *Cell* **2012**, *150*, 1121-1134, doi:10.1016/j.cell.2012.08.024.
18. Okudela, K.; Suzuki, M.; Kageyama, S.; Bunai, T.; Nagura, K.; Igarashi, H.; Takamochi, K.; Suzuki, K.; Yamada, T.; Niwa, H., et al. PIK3CA mutation and amplification in human lung cancer. *Pathol Int* **2007**, *57*, 664-671, doi:10.1111/j.1440-1827.2007.02155.x.
19. Soria, J.C.; Lee, H.Y.; Lee, J.I.; Wang, L.; Issa, J.P.; Kemp, B.L.; Liu, D.D.; Kurie, J.M.; Mao, L.; Khuri, F.R. Lack of PTEN expression in non-small cell lung cancer could be related to promoter methylation. *Clin Cancer Res* **2002**, *8*, 1178-1184.
20. Spoerke, J.M.; O'Brien, C.; Huw, L.; Koeppen, H.; Fridlyand, J.; Brachmann, R.K.; Haverty, P.M.; Pandita, A.; Mohan, S.; Sampath, D., et al. Phosphoinositide 3-kinase (PI3K) pathway alterations are associated with histologic subtypes and are predictive of sensitivity to PI3K inhibitors in lung cancer preclinical models. *Clin Cancer Res* **2012**, *18*, 6771-6783, doi:10.1158/1078-0432.CCR-12-2347.
21. Rekhtman, N.; Paik, P.K.; Arcila, M.E.; Tafe, L.J.; Oxnard, G.R.; Moreira, A.L.; Travis, W.D.; Zakowski, M.F.; Kris, M.G.; Ladanyi, M. Clarifying the spectrum of driver oncogene mutations in biomarker-verified squamous carcinoma of lung: lack of EGFR/KRAS and presence of PIK3CA/AKT1 mutations. *Clin Cancer Res* **2012**, *18*, 1167-1176, doi:10.1158/1078-0432.CCR-11-2109.
22. Lindeman, N.I.; Cagle, P.T.; Aisner, D.L.; Arcila, M.E.; Beasley, M.B.; Bernicker, E.H.; Colasacco, C.; Dacic, S.; Hirsch, F.R.; Kerr, K., et al. Updated Molecular Testing Guideline for the Selection of Lung Cancer Patients for Treatment With Targeted Tyrosine Kinase Inhibitors: Guideline From the College of American Pathologists, the International Association for the Study of Lung Cancer, and the Association for Molecular Pathology. *Arch Pathol Lab Med* **2018**, *142*, 321-346, doi:10.5858/arpa.2017-0388-CP.
23. Sands, J.M.; Nguyen, T.; Shivdasani, P.; Sacher, A.G.; Cheng, M.L.; Alden, R.S.; Janne, P.A.; Kuo, F.C.; Oxnard, G.R.; Sholl, L.M. Next-generation sequencing informs diagnosis and identifies unexpected therapeutic targets in lung squamous cell carcinomas. *Lung Cancer* **2020**, *140*, 35-41, doi:10.1016/j.lungcan.2019.12.005.
24. Janku, F.; Yap, T.A.; Meric-Bernstam, F. Targeting the PI3K pathway in cancer: are we making headway? *Nature reviews. Clinical oncology* **2018**, *15*, 273-291, doi:10.1038/nrclinonc.2018.28.
25. Sabatini, D.M. mTOR and cancer: insights into a complex relationship. *Nat Rev Cancer* **2006**, *6*, 729-734, doi:10.1038/nrc1974.
26. Kim, L.C.; Cook, R.S.; Chen, J. mTORC1 and mTORC2 in cancer and the tumor microenvironment. *Oncogene* **2017**, *36*, 2191-2201, doi:10.1038/onc.2016.363.
27. Guertin, D.A.; Sabatini, D.M. Defining the role of mTOR in cancer. *Cancer Cell* **2007**, *12*, 9-22, doi:10.1016/j.ccr.2007.05.008.
28. Martin, J.; Masri, J.; Bernath, A.; Nishimura, R.N.; Gera, J. Hsp70 associates with Rictor and is required for mTORC2 formation and activity. *Biochem Biophys Res Commun* **2008**, *372*, 578-583, doi:10.1016/j.bbrc.2008.05.086.
29. Xie, J.; Proud, C.G. Signaling crosstalk between the mTOR complexes. *Translation (Austin)* **2014**, *2*, e28174, doi:10.4161/trla.28174.
30. Dan, H.C.; Adli, M.; Baldwin, A.S. Regulation of mammalian target of rapamycin activity in PTEN-inactive prostate cancer cells by I kappa B kinase alpha. *Cancer Res* **2007**, *67*, 6263-6269, doi:10.1158/0008-5472.CAN-07-1232.

31. Gkountakos, A.; Pilotto, S.; Mafficini, A.; Vicentini, C.; Simbolo, M.; Milella, M.; Tortora, G.; Scarpa, A.; Bria, E.; Corbo, V. Unmasking the impact of Rictor in cancer: novel insights of mTORC2 complex. *Carcinogenesis* **2018**, *39*, 971-980, doi:10.1093/carcin/bgy086.
32. Saxton, R.A.; Sabatini, D.M. mTOR Signaling in Growth, Metabolism, and Disease. *Cell* **2017**, *169*, 361-371, doi:10.1016/j.cell.2017.03.035.
33. Manning, B.D.; Toker, A. AKT/PKB Signaling: Navigating the Network. *Cell* **2017**, *169*, 381-405, doi:10.1016/j.cell.2017.04.001.
34. Sarbassov, D.D.; Ali, S.M.; Kim, D.H.; Guertin, D.A.; Latek, R.R.; Erdjument-Bromage, H.; Tempst, P.; Sabatini, D.M. Rictor, a novel binding partner of mTOR, defines a rapamycin-insensitive and raptor-independent pathway that regulates the cytoskeleton. *Curr Biol* **2004**, *14*, 1296-1302, doi:10.1016/j.cub.2004.06.054.
35. Dibble, C.C.; Asara, J.M.; Manning, B.D. Characterization of Rictor phosphorylation sites reveals direct regulation of mTOR complex 2 by S6K1. *Mol Cell Biol* **2009**, *29*, 5657-5670, doi:10.1128/MCB.00735-09.
36. Boulbes, D.; Chen, C.H.; Shaikenov, T.; Agarwal, N.K.; Peterson, T.R.; Addona, T.A.; Keshishian, H.; Carr, S.A.; Magnuson, M.A.; Sabatini, D.M., et al. Rictor phosphorylation on the Thr-1135 site does not require mammalian target of rapamycin complex 2. *Mol Cancer Res* **2010**, *8*, 896-906, doi:10.1158/1541-7786.MCR-09-0409.
37. Sarbassov, D.D.; Guertin, D.A.; Ali, S.M.; Sabatini, D.M. Phosphorylation and regulation of Akt/PKB by the rictor-mTOR complex. *Science* **2005**, *307*, 1098-1101, doi:10.1126/science.1106148.
38. Hresko, R.C.; Mueckler, M. mTOR.RICTOR is the Ser473 kinase for Akt/protein kinase B in 3T3-L1 adipocytes. *J Biol Chem* **2005**, *280*, 40406-40416, doi:10.1074/jbc.M508361200.
39. Dancey, J. mTOR signaling and drug development in cancer. *Nat Rev Clin Oncol* **2010**, *7*, 209-219, doi:10.1038/nrclinonc.2010.21.
40. Breuleux, M.; Klopfenstein, M.; Stephan, C.; Doughty, C.A.; Barys, L.; Maira, S.M.; Kwiatkowski, D.; Lane, H.A. Increased AKT S473 phosphorylation after mTORC1 inhibition is rictor dependent and does not predict tumor cell response to PI3K/mTOR inhibition. *Mol Cancer Ther* **2009**, *8*, 742-753, doi:10.1158/1535-7163.MCT-08-0668.
41. Wu, M.J.; Chang, C.H.; Chiu, Y.T.; Wen, M.C.; Shu, K.H.; Li, J.R.; Chiu, K.Y.; Chen, Y.T. Rictor-dependent AKT activation and inhibition of urothelial carcinoma by rapamycin. *Urol Oncol* **2012**, *30*, 69-77, doi:10.1016/j.urolonc.2009.11.009.
42. Guertin, D.A.; Stevens, D.M.; Thoreen, C.C.; Burds, A.A.; Kalaany, N.Y.; Moffat, J.; Brown, M.; Fitzgerald, K.J.; Sabatini, D.M. Ablation in mice of the mTORC components raptor, rictor, or mLST8 reveals that mTORC2 is required for signaling to Akt-FOXO and PKCalpha, but not S6K1. *Dev Cell* **2006**, *11*, 859-871, doi:10.1016/j.devcel.2006.10.007.
43. Shiota, C.; Woo, J.T.; Lindner, J.; Shelton, K.D.; Magnuson, M.A. Multiallelic disruption of the rictor gene in mice reveals that mTOR complex 2 is essential for fetal growth and viability. *Dev Cell* **2006**, *11*, 583-589, doi:10.1016/j.devcel.2006.08.013.
44. Thomanetz, V.; Angliker, N.; Cloetta, D.; Lustenberger, R.M.; Schweighauser, M.; Oliveri, F.; Suzuki, N.; Ruegg, M.A. Ablation of the mTORC2 component rictor in brain or Purkinje cells affects size and neuron morphology. *J Cell Biol* **2013**, *201*, 293-308, doi:10.1083/jcb.201205030.

45. Ravichandran, K.; Zafar, I.; He, Z.; Doctor, R.B.; Moldovan, R.; Mullick, A.E.; Edelstein, C.L. An mTOR anti-sense oligonucleotide decreases polycystic kidney disease in mice with a targeted mutation in Pkd2. *Hum Mol Genet* **2014**, *23*, 4919-4931, doi:10.1093/hmg/ddu208.
46. Jia, W.; Sanders, A.J.; Jia, G.; Liu, X.; Lu, R.; Jiang, W.G. Expression of the mTOR pathway regulators in human pituitary adenomas indicates the clinical course. *Anticancer Res* **2013**, *33*, 3123-3131.
47. Cheng, H.; Zou, Y.; Ross, J.S.; Wang, K.; Liu, X.; Halmos, B.; Ali, S.M.; Liu, H.; Verma, A.; Montagna, C., et al. RICTOR Amplification Defines a Novel Subset of Patients with Lung Cancer Who May Benefit from Treatment with mTORC1/2 Inhibitors. *Cancer Discov* **2015**, *5*, 1262-1270, doi:10.1158/2159-8290.CD-14-0971.
48. Simbolo, M.; Mafficini, A.; Sikora, K.O.; Fassan, M.; Barbi, S.; Corbo, V.; Mastracci, L.; Rusev, B.; Grillo, F.; Vicentini, C., et al. Lung neuroendocrine tumours: deep sequencing of the four World Health Organization histotypes reveals chromatin-remodelling genes as major players and a prognostic role for TERT, RB1, MEN1 and KMT2D. *J Pathol* **2017**, *241*, 488-500, doi:10.1002/path.4853.
49. Ross, J.S.; Wang, K.; Elkadi, O.R.; Tarasen, A.; Foulke, L.; Sheehan, C.E.; Otto, G.A.; Palmer, G.; Yelensky, R.; Lipson, D., et al. Next-generation sequencing reveals frequent consistent genomic alterations in small cell undifferentiated lung cancer. *J Clin Pathol* **2014**, *67*, 772-776, doi:10.1136/jclinpath-2014-202447.
50. Umemura, S.; Mimaki, S.; Makinoshima, H.; Tada, S.; Ishii, G.; Ohmatsu, H.; Niho, S.; Yoh, K.; Matsumoto, S.; Takahashi, A., et al. Therapeutic priority of the PI3K/AKT/mTOR pathway in small cell lung cancers as revealed by a comprehensive genomic analysis. *J Thorac Oncol* **2014**, *9*, 1324-1331, doi:10.1097/JTO.0000000000000250.
51. Sakre, N.; Wildey, G.; Behtaj, M.; Kresak, A.; Yang, M.; Fu, P.; Dowlati, A. RICTOR amplification identifies a subgroup in small cell lung cancer and predicts response to drugs targeting mTOR. *Oncotarget* **2017**, *8*, 5992-6002, doi:10.18632/oncotarget.13362.
52. Wang, S.; Song, X.; Li, X.; Zhao, X.; Chen, H.; Wang, J.; Wu, J.; Gao, Z.; Qian, J.; Han, B., et al. RICTOR polymorphisms affect efficiency of platinum-based chemotherapy in Chinese non-small-cell lung cancer patients. *Pharmacogenomics* **2016**, *17*, 1637-1647, doi:10.2217/pgs-2016-0070.
53. Krencz, I.; Sebestyen, A.; Fabian, K.; Mark, A.; Moldvay, J.; Khoor, A.; Kopper, L.; Papay, J. Expression of mTORC1/2-related proteins in primary and brain metastatic lung adenocarcinoma. *Hum Pathol* **2017**, *62*, 66-73, doi:10.1016/j.humpath.2016.12.012.
54. Pilotto, S.; Simbolo, M.; Sperduti, I.; Novello, S.; Vicentini, C.; Peretti, U.; Pedron, S.; Ferrara, R.; Caccese, M.; Milella, M., et al. OA06.06 Druggable Alterations Involving Crucial Carcinogenesis Pathways Drive the Prognosis of Squamous Cell Lung Carcinoma (SqCLC). *Journal of Thoracic Oncology 12*, S266-S267, doi:10.1016/j.jtho.2016.11.260.
55. Simbolo, M.; Gottardi, M.; Corbo, V.; Fassan, M.; Mafficini, A.; Malpeli, G.; Lawlor, R.T.; Scarpa, A. DNA qualification workflow for next generation sequencing of histopathological samples. *PLoS One* **2013**, *8*, e62692, doi:10.1371/journal.pone.0062692.
56. Zamo, A.; Bertolaso, A.; van Raaij, A.W.; Mancini, F.; Scardoni, M.; Montresor, M.; Menestrina, F.; van Krieken, J.H.; Chilosi, M.; Groenen, P.J., et al. Application

of microfluidic technology to the BIOMED-2 protocol for detection of B-cell clonality. *J Mol Diagn* **2012**, *14*, 30-37, doi:10.1016/j.jmoldx.2011.07.007.
57. Zheng, C.X.; Gu, Z.H.; Han, B.; Zhang, R.X.; Pan, C.M.; Xiang, Y.; Rong, X.J.; Chen, X.; Li, Q.Y.; Wan, H.Y. Whole-exome sequencing to identify novel somatic mutations in squamous cell lung cancers. *Int J Oncol* **2013**, *43*, 755-764, doi:10.3892/ijo.2013.1991.
58. Kim, Y.; Hammerman, P.S.; Kim, J.; Yoon, J.A.; Lee, Y.; Sun, J.M.; Wilkerson, M.D.; Pedamallu, C.S.; Cibulskis, K.; Yoo, Y.K., et al. Integrative and comparative genomic analysis of lung squamous cell carcinomas in East Asian patients. *J Clin Oncol* **2014**, *32*, 121-128, doi:10.1200/JCO.2013.50.8556.
59. Yin, S.; Yang, J.; Lin, B.; Deng, W.; Zhang, Y.; Yi, X.; Shi, Y.; Tao, Y.; Cai, J.; Wu, C.I., et al. Exome sequencing identifies frequent mutation of MLL2 in non-small cell lung carcinoma from Chinese patients. *Sci Rep* **2014**, *4*, 6036, doi:10.1038/srep06036.
60. Cingolani, P.; Patel, V.M.; Coon, M.; Nguyen, T.; Land, S.J.; Ruden, D.M.; Lu, X. Using Drosophila melanogaster as a Model for Genotoxic Chemical Mutational Studies with a New Program, SnpSift. *Front Genet* **2012**, *3*, 35, doi:10.3389/fgene.2012.00035.
61. McLaren, W.; Pritchard, B.; Rios, D.; Chen, Y.; Flicek, P.; Cunningham, F. Deriving the consequences of genomic variants with the Ensembl API and SNP Effect Predictor. *Bioinformatics* **2010**, *26*, 2069-2070, doi:10.1093/bioinformatics/btq330.
62. Robinson, J.T.; Thorvaldsdottir, H.; Winckler, W.; Guttman, M.; Lander, E.S.; Getz, G.; Mesirov, J.P. Integrative genomics viewer. *Nat Biotechnol* **2011**, *29*, 24-26, doi:10.1038/nbt.1754.